

TCS Ni-based Superalloys Database (TCNI)

Examples Collection



Contents

About the Database Examples	3
TCS Ni-based Superalloys Database (TCNI) Resources	4
TCNI Validation Examples	5
Pseudo-binary Phase Diagram	6
Prediction of Phase Stability	7
Predicting Phase Stability: Applications Involving P	9
Property Predictions	13
Treatment Predictions	16
Al-Hf-Ni Liquidus Solidus and Isolethal Section	17
Solute Partition Coefficient for Ni-base Alloys	19
Isothermal Solidification During Brazing: A Diffusion Simulation	20
Surface Tension of CMSX-10 Superalloy	22
Viscosity of CMSX-10 Superalloy	24
Electrical Resistivity of Some Commercial Alloys	26
Thermal Conductivity of Some Commercial Alloys	28
TCNI Calculation Examples	30
Binary Phase Diagrams	31
Ternary Isothermal Phase Diagram Sections	33
Prediction of Stable Phases	36
Prediction of Phase Stability with Minor Amounts of P in Ni-base Superalloys	38
Heat Treatment of a GTD111 Alloy	40
Precipitation and Coarsening of a 718 Alloy	42
Surface Tension: Cu-Fe, Fe-Ni, Cu-Ni, and Cu-Fe-Ni	45
Viscosity: Fe-Ni, Cr-Ni, and Cr-Fe-Ni	48
Electrical Resistivity: Co-Ni, Co-Fe, Co-Fe-Ni, and Higher Order Systems	51
Thermal Conductivity: Co-Ni, Co-Fe, and Co-Fe-Ni	54

About the Database Examples

There are examples available to demonstrate both the *validity* of the database itself as well as to demonstrate some of its *calculation* capabilities when combined with Thermo-Calc software and its Add-on Modules and features.



For each database, the type and number of available examples varies. In some cases an example can belong to both a validation and calculation type.

- *Validation* examples generally include experimental data in the plot or diagram to show how close to the predicted data sets the Thermo-Calc calculations are. It uses the most recent version of the software and relevant database(s) unless otherwise specified.
- *Calculation* examples are intended to demonstrate a use case of the database. This might be showing a binary or ternary system calculated in a phase diagram, or demonstrate how the database and relevant software features would be applied to a heat treatment application, process metallurgy, soldering process, and so forth. In the case of heat treatment, it might include the result of calculating solidification segregation, determining homogenization temperature and then predicting the time needed to homogenize. There are many other examples specifically related to each database.



Where relevant, most references related to each example set are included at the end of the individual section. You can also find additional references specific to the database itself when using the database within Thermo-Calc. You can also contact us directly should you have any questions.



If you are interested in sharing your own examples using Thermo-Calc products in unique or surprising ways, or if you want to share your results from a peer reviewed paper, send an email to info@thermocalc.com.

TCS Ni-based Superalloys Database (TCNI) Resources

Information about the database is available on our website and in the Thermo-Calc software online Help.

- **Website:** On our website the information is both searchable and the database specific PDFs are available to download.
- **Online Help:** Technical database information is included with the Thermo-Calc software online Help. When in Thermo-Calc, press F1 to search for the same information as is contained in the PDF documents described. Depending on the database, there are additional examples available on the website.

Database Specific Documentation

- The *TCS Ni-based Superalloys Database (TCNI) Technical Information* PDF document contains version specific information such as the binary and ternary assessed systems, phases, models, and properties data. It also includes details about the properties data (e.g. viscosity, surface tension, etc.), a list of the included elements, and summaries of the database revision history by version.
- The *TCS Ni-based Superalloys Database (TCNI) Examples Collection* PDF document contains a series of validation examples using experimental data and a set of calculation examples showing some of the ways the database can generally be used.



Go to the [Nickel-based Superalloys Databases](#) page on our website where you can access an examples collection and the technical information plus learn more about the compatible kinetic database. Also explore further [applications of Thermo-Calc to nickel](#) including links to resources such as examples, publications, and more.



Learn more on our website about the [CALPHAD Method](#) and how it is applied to the Thermo-Calc databases.

TCNI Validation Examples



Some of these phase diagrams are calculated with earlier versions of the database, so negligible differences might be observed if these are recalculated with the most recent version. The diagrams are updated where there is considerable or significant improvements.

In this section:

Pseudo-binary Phase Diagram	6
Prediction of Phase Stability	7
Predicting Phase Stability: Applications Involving P	9
Property Predictions	13
Treatment Predictions	16
Al-Hf-Ni Liquidus Solidus and Isolethal Section	17
Solute Partition Coefficient for Ni-base Alloys	19
Isothermal Solidification During Brazing: A Diffusion Simulation	20
Surface Tension of CMSX-10 Superalloy	22
Viscosity of CMSX-10 Superalloy	24
Electrical Resistivity of Some Commercial Alloys	26
Thermal Conductivity of Some Commercial Alloys	28

Pseudo-binary Phase Diagram

This example using the TCS Ni-based Superalloys Database (TCNI) is a type of calculated isoplethal phase diagram section of a ternary system called a pseudo-binary, meaning that the section lies precisely in the plane of constant potentials (meaning along tie-lines). It is compared with literature data.

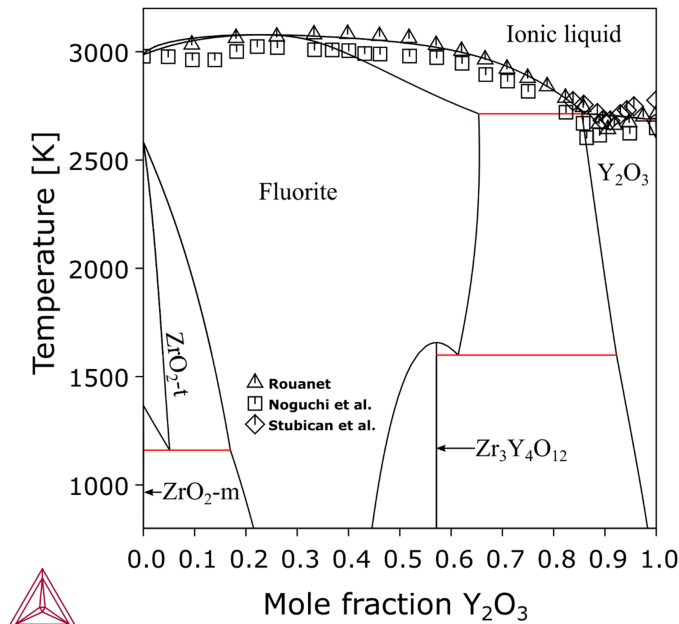


Figure 1: Section ZrO_2 - Y_2O_3 compared with experimental data [1968Rou; 1970Nog; 1978Stu].

References

- [1968Rou] A. Rouanet, High-temperature solidification and phase diagrams of the ZrO_2 - Er_2O_3 , ZrO_2 - Y_2O_3 , and ZrO_2 - Yb_2O_3 systems (Diagrammes de solidification et diagrammes de phases de haute temperature des systemes zircone-oxyde d'erbium, zircone-oxyde d'yttrium et. Comptes Rendus l'Academie des Sci. Ser. C Chem. 267, 1581-1584 (1968).
- [1970Nog] T. Noguchi, M. Mizuno, T. Yamada, The Liquidus Curve of the ZrO_2 - Y_2O_3 System as Measured by a Solar Furnace. Bull. Chem. Soc. Jpn. 43, 2614-2616 (1970).
- [1978Stu] V. S. Stubican, R. C. Hink, S. P. Ray, Phase Equilibria and Ordering in the System ZrO_2 - Y_2O_3 . J. Am. Ceram. Soc. 61, 17-21 (1978).

Prediction of Phase Stability

The TCS Ni-based Superalloys Database (TCNI) is routinely validated against industrial alloy data in order to make sure alloys are still well described with each new released database version.

The following example plots represent common usage examples, where the equilibrium and metastable phases present in an alloy are calculated with the variation of temperature.

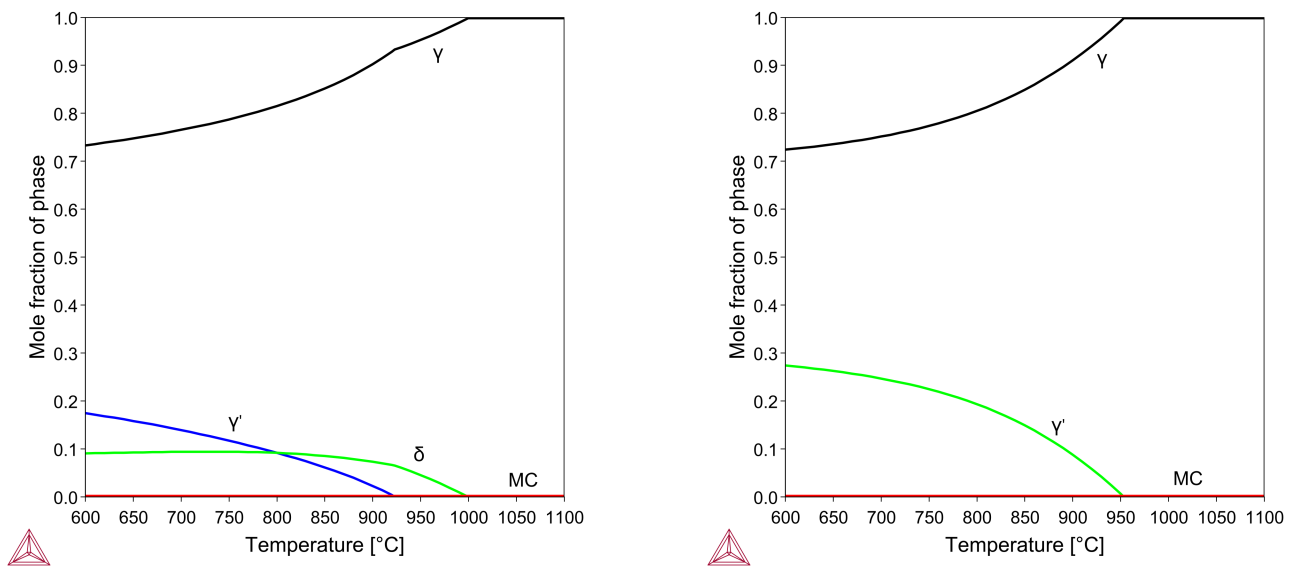


Figure 2: Predicted amount of phases at varying temperatures for a Ni-18Cr-10Fe-9Co-2.8Mo-1.5Al-0.7Ti-5.3Nb-0.02C (wt. %) alloy, (left) stable phases and (right) metastable phases. Delta (δ) phase solvus measured in the range 1000-1020 °C and the metastable γ' solvus measured at 963 °C.

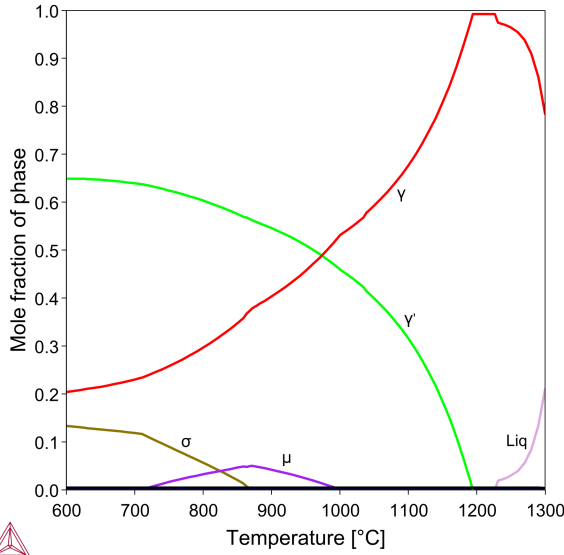


Figure 3: Predicted amount of phases at varying temperatures for a Ni-11.5Cr-15.5Co-6.5Mo-4.3Al-4.3Ti-0.5Hf (wt. %) alloy. Experimental γ' solvus temperature in the literature is close to 1191 °C and both σ and μ phases were observed at 760 °C after 1000 hours heat treatment.

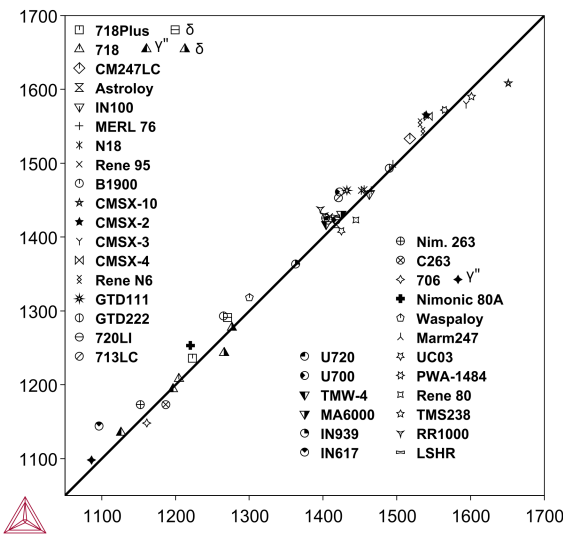


Figure 4: Calculated precipitate solvus temperature for various Ni-base superalloys compared with literature data (γ' L₂ unless other precipitate specified in the legend).

Predicting Phase Stability: Applications Involving P

These examples using the TCS Ni-based Superalloys Database (TCNI) include the use of the recently added element, phosphorus (P). The example is also an overview of the use of the different calculation types available: Material to Material Calculator, Diffusion Calculator, and Scheil Calculator.



For other examples using P, see [Prediction of Phase Stability with Minor Amounts of P in Ni-base Superalloys](#) and [Isothermal Solidification During Brazing: A Diffusion Simulation](#).

Predicting Phase Stability with the Material to Material Calculator

The Material to Material Calculator, which is available for all Thermo-Calc users, allows for a straightforward prediction of phase diagrams with a composition varying between two materials.



Read more on our website about the [Material to Material Calculator](#). If you are in Thermo-Calc, press F1 to search the help.

The following shows the predicted stable phases with varying mass fraction of Ni-11P (BNi-6) filler mixed with Ni-base alloy GH3039 (Ni-15Cr-1.4Fe-1.7Mo-0.7Nb-0.3Ti-0.5Al-0.08C). In [Figure 5](#), the far left edge represents pure GH3039, and the far right represents pure BNi-6. The red line represents the liquidus of the alloy. We can expect that while cooling, and if there is any liquid filler left in the joint, then it might form a microstructure of $\gamma + Ni_3P$.

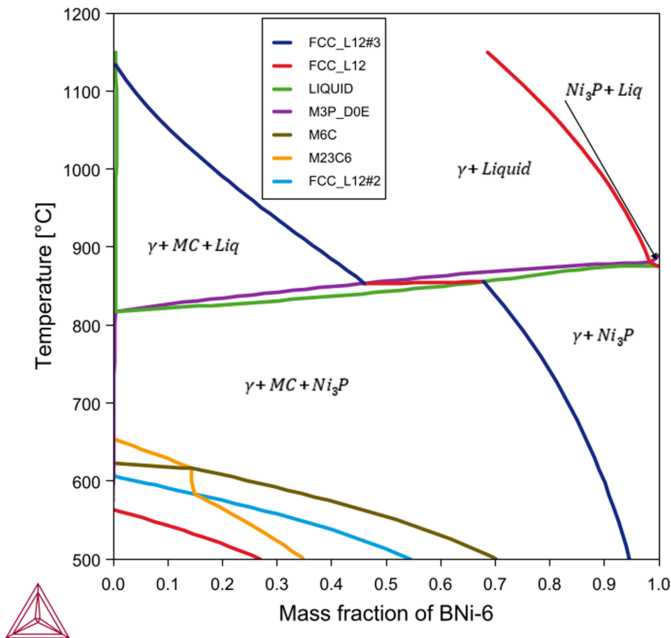


Figure 5: A material-to-material calculation mixing a Ni-base alloy GH3039 with a brazing filler BNi-6. Labels show which phase is formed or disappears while passing through a line.

Predicting Phase Stability with the Diffusion Module (DICTRA)

In the next example, both the thermodynamic TCS Ni-based Superalloys Database (TCNI) and its compatible kinetic TCS Ni-alloys Mobility Database (MOBNI) are used with the Add-on Diffusion Module (DICTRA) to further examine the set up started with the Material to Material Calculator. The Diffusion Module (DICTRA) requires an additional license although all users can use a demonstration version with up to three components.



Read more about the [Diffusion Module \(DICTRA\)](#) on our website. If you are in Thermo-Calc, press F1 to search the help to learn about the available settings included with the Add-on Module.

A simplified diffusion simulation of this example, representing GH3039 with Ni-15Cr, results in the composition profiles shown in [Figure 6](#). A brazing at 1050 °C for 20 minutes is simulated.



The experimental data points in [Figure 6](#) are measured on the final microstructure of the joint; effects during solidification affects the data. Moreover, there are discrepancies between the predicted and measured compositions because the simulation excludes some elements.

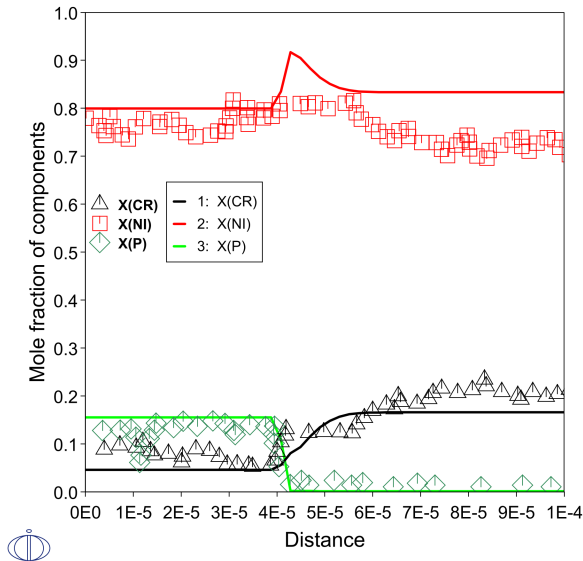


Figure 6: Final composition profile after simulation of interdiffusion between Ni-11P (left side) and Ni-15Cr (right side). Experimental data from the literature, measured on final microstructure [2021Lv].

Predicting Phase Stability with the Scheil Calculator

In addition to diffusion calculations with the DICTRA module (in Console Mode) or the Diffusion Calculator (in Graphical Mode), you can also add Scheil solidification calculations to further investigate the prediction of phase stability. In Graphical Mode, the Scheil Calculator is used and in Console Mode the Scheil module.



Read more about [Scheil Solidification Simulations](#) on our website. If you are in Thermo-Calc, press F1 to search the help to learn about using Scheil.

After the diffusion calculations, you can next take the composition in the center of the filler, i.e. a region that is still liquid at the end of brazing, and perform a Scheil solidification simulation to see which phases are predicted to precipitate during rapid cooling of the joint.

After setting up the simulation to use the Scheil Calculator with Thermo-Calc, [Figure 7](#) shows the mole fraction of solid as temperature decreases from 1050 °C. There is a rather slow, primary precipitation of γ (FCC_A1) between 1050 °C and 871 °C, after which most of the liquid is rapidly solidified as $\gamma + Ni_3P$ under the eutectic temperature.

This is in good agreement with the general appearance of the phase diagram predicted by the Material to Material Calculator, especially if you look at the right-hand side of [Figure 5](#) where there is some mixing of filler with the parent metal.

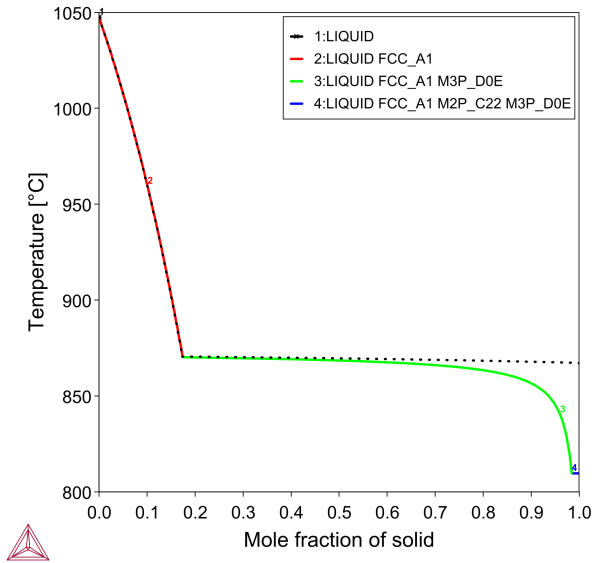


Figure 7: Mole fraction of solid as temperature decreases from 1050 °C.

Reference

[2021Lv] Y. Lv, K. Han, T. Wang, Effect of brazing temperature on the interfacial microstructure and mechanical properties of GH3039 joint brazed with electroless Ni-P filler metal. *Weld. World*. 65, 2221–2229 (2021).

Property Predictions

The TCS Ni-based Superalloys Database (TCNI) database is validated against experimental data of phase composition, and other properties related to the molar volume of phases.

Table 1. Predicted compositions of γ and γ' as well as the fraction in two Ni-base alloys compared with measurements (in brackets) from the literature [2008Sud].

at. %	Ni	Al	Cr	W	Experimental γ' fraction	Predicted γ' fraction
Ni-9.8Al-8.3Cr γ	82.9 (82.7)	8.51 (8.43)	8.61 (8.86)	-		
Ni-9.8Al-8.3Cr γ'	76.7 (76.6)	16.7 (17.4)	6.63 (5.99)	-	18.9	15.8
Ni-9.7Al-8.5Cr-2W γ	81.5 (81.8)	6.75(6.23)	9.66(10.48)	2.06 (1.54)		
Ni-9.7Al-8.5Cr-2W γ'	76.4 (76.2)	15.5 (16.9)	6.24 (3.94)	1.87 (3.00)	30.8	33.9

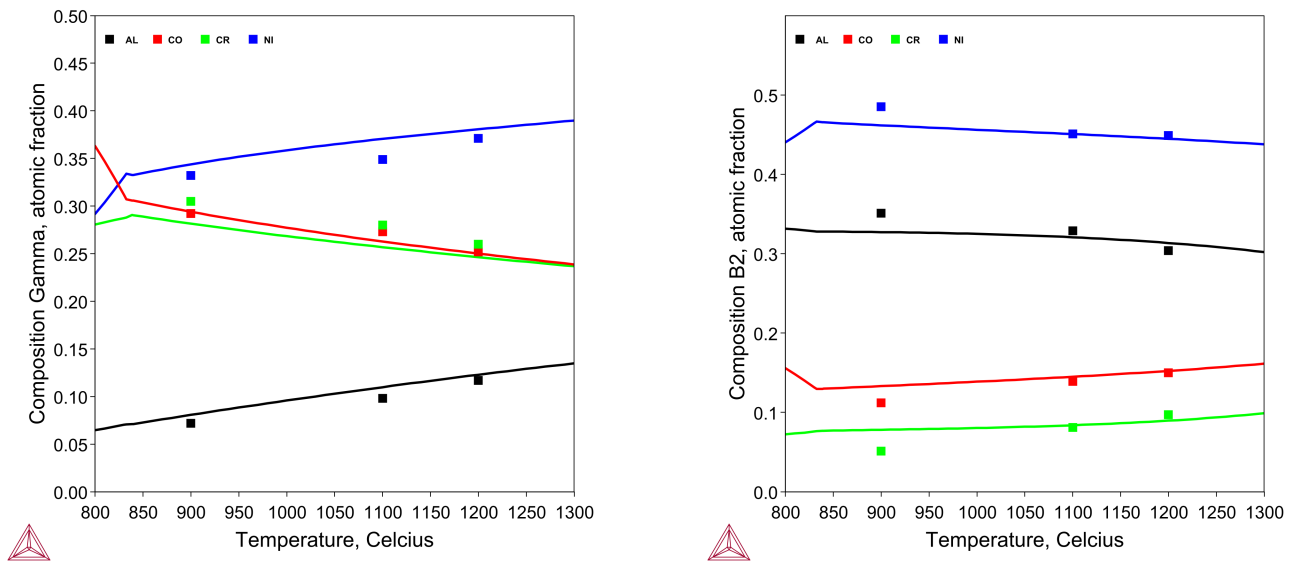


Figure 8: Composition of the (left) γ -A1 and (right) β -B2 phases of Ni-24Al-15Cr-19Co alloy calculated and measured by EPMA [2015Ghe].

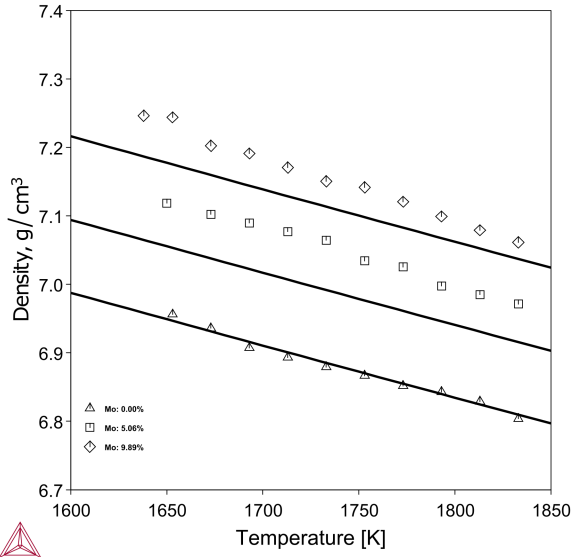


Figure 9: Predicted densities of liquid Ni-Cr-Al-Mo alloys where the molar ratio of Ni:Cr:Al is close to the average value for commercial superalloys INCO713, CM247LC, and CMSX-4. Symbols are experimental values from the literature [2006Fan].

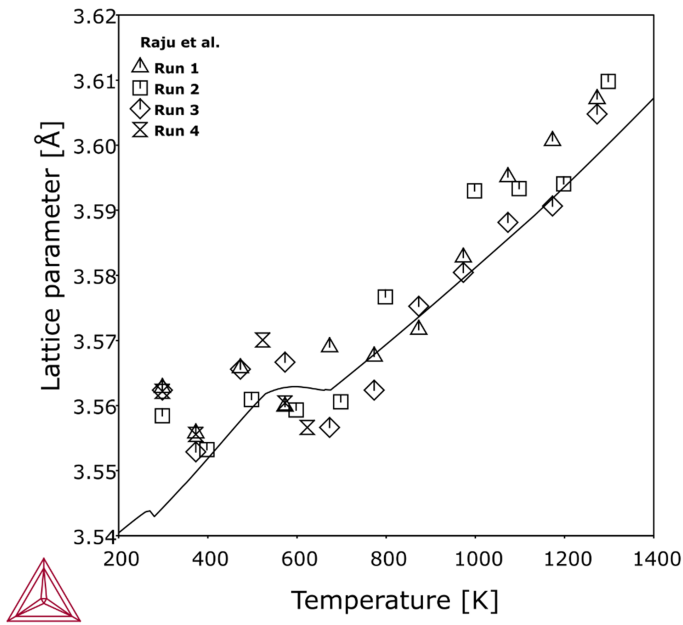


Figure 10: Predicted lattice parameters of disordered FCC of Inconel 600 at varying temperatures compared to X-ray diffraction data [2004Raj]. At low temperature the calculation gives, besides the disordered FCC, also an ordered L12 phase, which causes the kink in the curve.

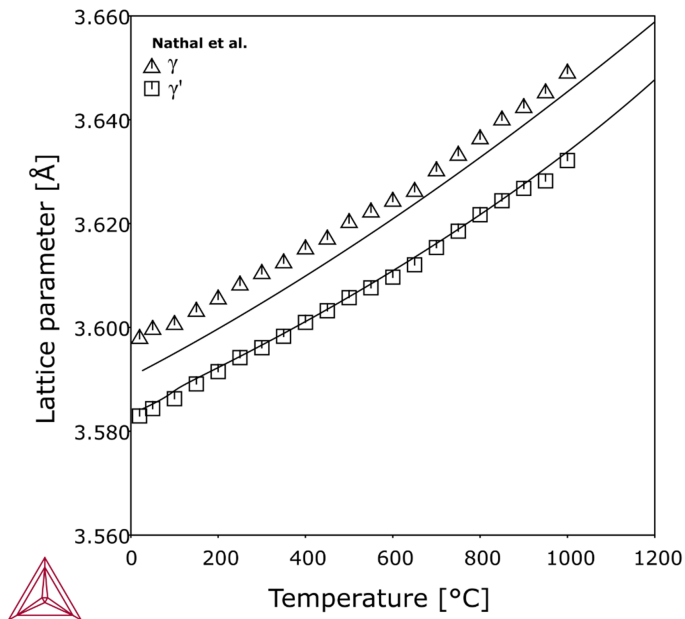


Figure 11: Predicted γ/γ' lattice mismatch of a Ni-0.6Mo-0.92Ta-12.5Al-1.83Ti-10.5Cr-3.3W (at. %) compared to experimental data [1985Nat].

References

- [1985Nat] M. V Nathal, R. A. Mackay, R. G. Garlick, Temperature dependence of γ - γ' lattice mismatch in Nickel-base superalloys. *Mater. Sci. Eng.* 75, 195–205 (1985).
- [2004Raj] S. Raju, K. Sivasubramanian, R. Divakar, G. Panneerselvam, A. Banerjee, E. Mohandas, M. . Antony, Thermal expansion studies on Inconel-600[®] by high temperature X-ray diffraction. *J. Nucl. Mater.* 325, 18–25 (2004).
- [2006Fan] L. Fang, Y. F. Wang, F. Xiao, Z. N. Tao, K. MuKai, Density of liquid NiCrAlMo quaternary alloys measured by a modified sessile drop method. *Mater. Sci. Eng. B.* 132, 164–169 (2006).
- [2008Sud] C. K. Sudbrack, T. D. Ziebell, R. D. Noebe, D. N. Seidman, Effects of a tungsten addition on the morphological evolution, spatial correlations and temporal evolution of a model Ni–Al–Cr superalloy. *Acta Mater.* 56, 448–463 (2008).
- [2015Ghe] T. Gheno, X. L. Liu, G. Lindwall, Z.-K. Liu, B. Gleeson, Experimental study and thermodynamic modeling of the Al–Co–Cr–Ni system. *Sci. Technol. Adv. Mater.* 16, 055001 (2015).

Treatment Predictions

The equilibrium conditions of heat treatments with the presence of gaseous species can also be predicted using the TCS Ni-based Superalloys Database (TCNI), for example oxidation or sulfidation treatments.

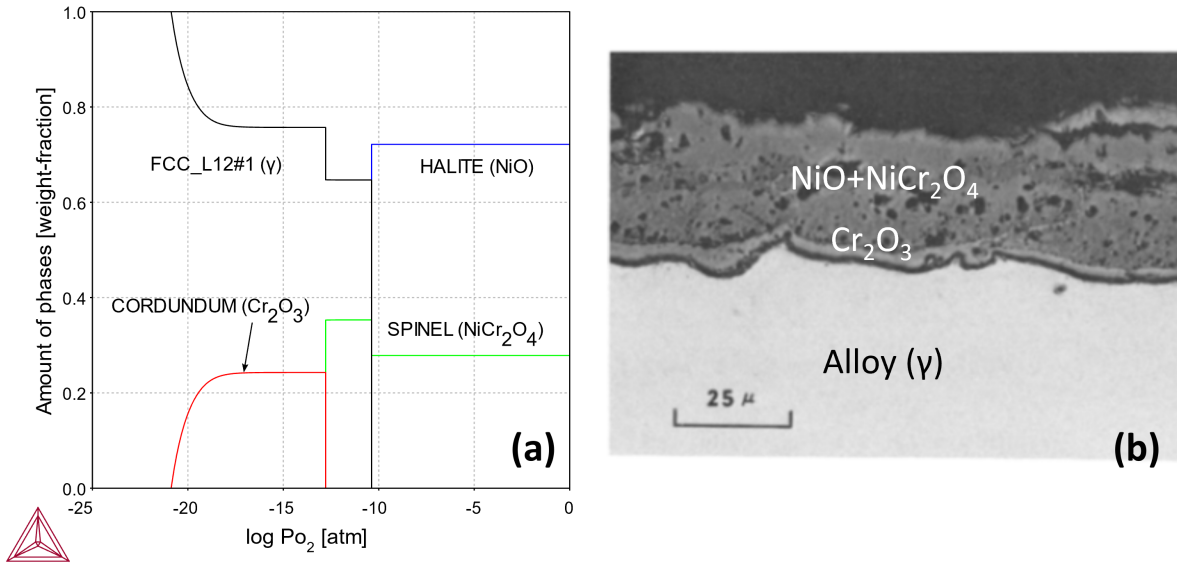


Figure 12: Oxide scale formed on Ni-18Cr alloy at 1000 °C (A) calculated (B) experiments for 20 hours in 1.0 atm O₂.

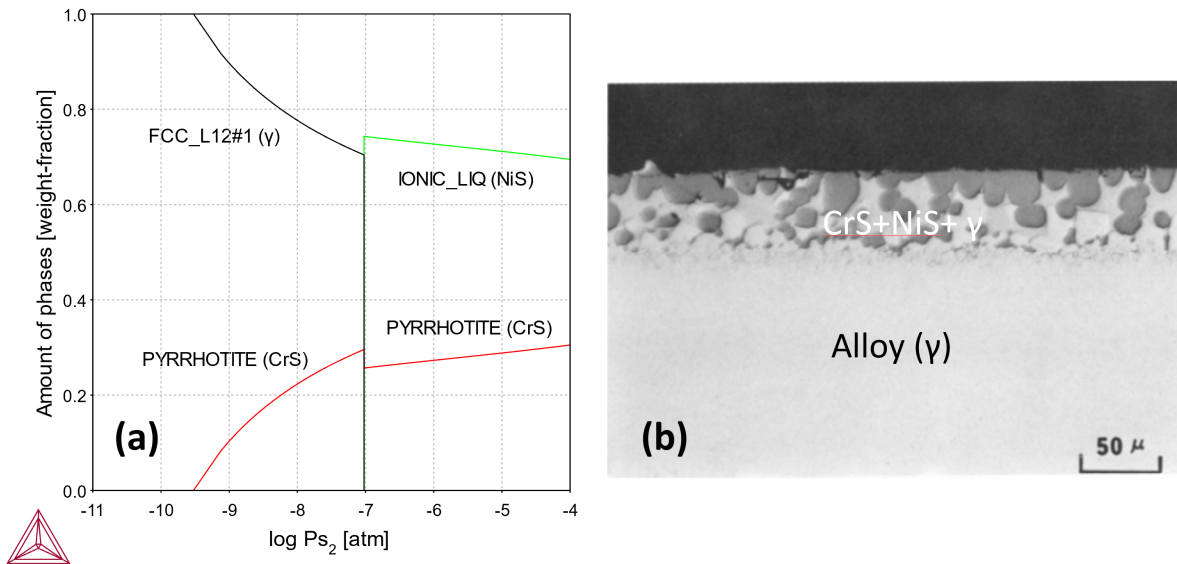


Figure 13: Sulfidized Ni-18Cr alloy at 1000 °C (A) calculated (B) experiments for 200 seconds in $aS=3.2e-3$. The surface sulfide layer contains particles of CrS (dark grey) and gamma-Ni (light) in a matrix of NiS.

Al-Hf-Ni Liquidus Solidus and Isolethal Section

These examples using the TCS Ni-based Superalloys Database (TCNI) show recent improvements to the Al-Hf-Ni system.

Liquidus Solidus

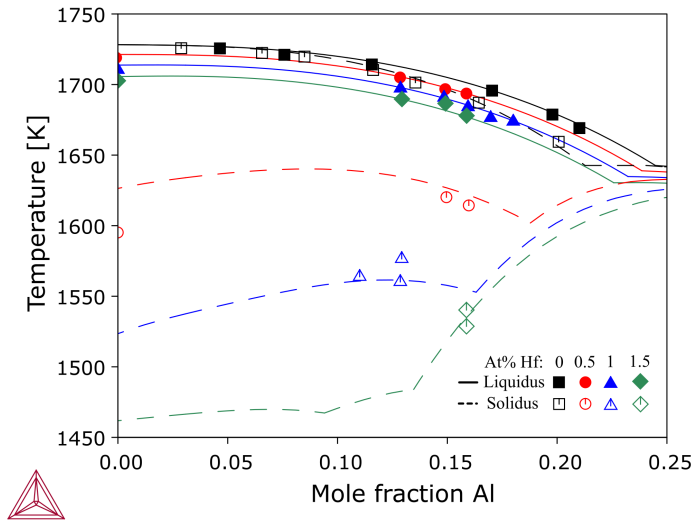


Figure 14: Calculated liquidus and solidus for Al-Hf-Ni with increasing Al-content, for varying amounts of Hf, compared with literature data [1999Miu].

Isolethal Section

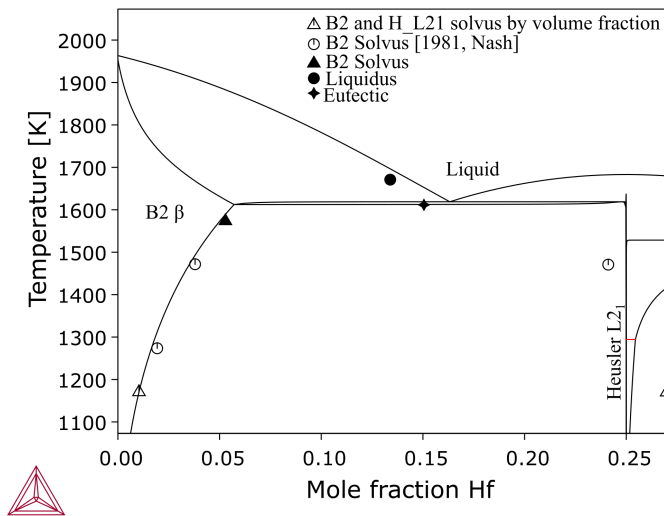


Figure 15: Calculated isoplethal section of Al-Hf-Ni system at 50 at% Ni compared with literature data: [1990Tak] unless otherwise specified [1981Nas].

References

- [1981Nas] P. Nash, D. R. F. West, Phase equilibria in Ni-rich region of Ni–Al–Hf system. *Met. Sci.* 15, 347–352 (1981).
- [1990Tak] M. Takeyama, C. T. Liu, Microstructures and mechanical properties of NiAl–Ni₂AlHf alloys. *J. Mater. Res.* 5, 1189–1196 (1990).
- [1999Miu] S. Miura, Y.-M. Hong, T. Suzuki, Y. Mishima, Liquidus and solidus temperatures of Ni-solid solution in Ni–Al–X (X: Ti, Zr, and Hf) ternary systems. *J. Phase Equilibria.* 20, 193–198 (1999).

Solute Partition Coefficient for Ni-base Alloys

The TCS Ni-based Superalloys Database (TCNI) can be used to show elemental partitioning in Ni-base alloys.

The partitioning coefficient represents the distribution of a solute element between two phases. Having well-predicted partitioning of elements between phases can be important in kinetic calculations, particularly certain Scheil calculations. The partitioning coefficient is calculated as $X(\text{phase 1, element}) / X(\text{phase 2, element})$.

Below is an example of calculated partitioning coefficients for Ni-base alloys, between the liquid and γ phase at the liquidus temperature, compared with data from the literature.

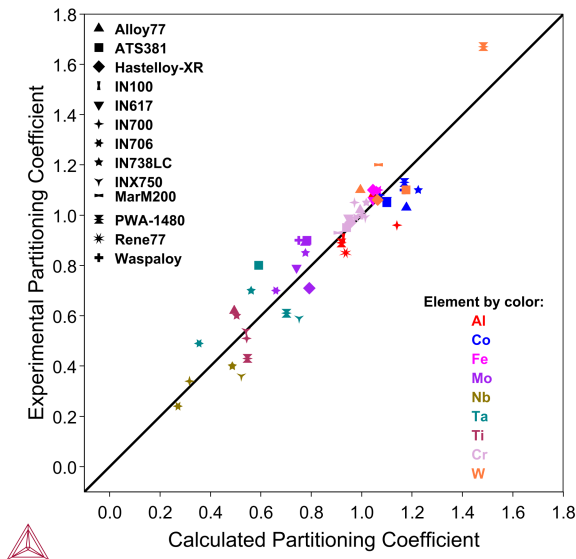


Figure 16: Calculated solute partitioning coefficient between FCC and liquid phase for numerous Ni-base alloys.

Isothermal Solidification During Brazing: A Diffusion Simulation

These examples using the TCS Ni-based Superalloys Database (TCNI) and TCS Ni-alloys Mobility Database (MOBNI) include the use of the recently added element, phosphorus (P).



For other examples using P, see [Prediction of Phase Stability with Minor Amounts of P in Ni-base Superalloys](#) and [Predicting Phase Stability: Applications Involving P](#).

Phosphorus is a common melt suppressant. It is sometimes preferred over boron in filler materials for transient liquid phase joining, also known as *brazing*, because the substitutional phosphorus has much lower solubility and mobility through the parent metal, thus it is harder for P to penetrate and supersaturate the parent metal and subsequently form embrittling precipitates out of the supersaturation.

The following example plots show the results from the Add-on Diffusion Module (DICTRA) simulation of Ni joined with a Ni-11P filler material, also known by the commercial name BNi-6. The Diffusion Module (DICTRA) requires an additional license although all users can use a demonstration version with up to three components.



Read more about the [Diffusion Module \(DICTRA\)](#) on our website. If you are in Thermo-Calc, press F1 to search the help to learn about the available settings included with the Add-on Module.

A simple setup is made of half of the experimental geometry, with one region representing half of the filler and one region representing one piece of parent Ni metal. This simulates the isothermal solidification during brazing at 1200 °C for 2.75 hours. Initially, mass balance promotes a rapid growth of the liquid filler region in the first timestep, and the region then shrinks as it solidifies at a rate proportional to the square root of the holding time. This liquid region size is known by measuring the *eutectic width* after cooling of the joint. Here the *grain boundary* diffusion model is used to emulate the enhanced penetration into the parent metal due to grain boundaries, as a function of grain size. In [Figure 17](#) and [Figure 18](#) it is shown that a smaller grain size, i.e. more grain boundaries, makes the liquid region shrink faster.



Grain boundary modeling is only available in Console Mode where you use the GB_MODEL command.

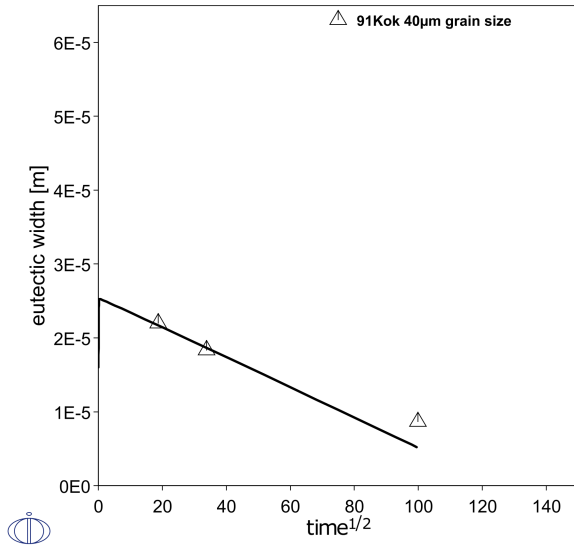


Figure 17: Simulated shrinkage of liquid brazing joint during isothermal solidification, with a parent FCC grain size of 40 μm [1991Kok].

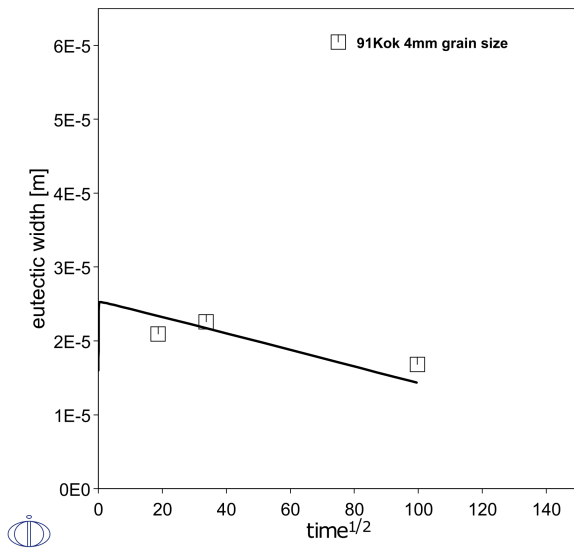


Figure 18: Simulated shrinkage of liquid brazing joint during isothermal solidification, with a parent FCC grain size of 4 mm [1991Kok].

Reference

[1991Kok] H. Kokawa, C. H. Lee, T. H. North, Effect of grain boundaries on isothermal solidification during transient liquid phase brazing. Metall. Trans. A. 22, 1627–1631 (1991).

Surface Tension of CMSX-10 Superalloy

The surface tension thermophysical property data is included with the TCS Ni-based Superalloys Database (TCNI) starting with version 10 (TCNI10).

For more information about the various thermophysical models, and when in Thermo-Calc, press F1 to search the online help. The details are found under a *General Reference* section.



You can find information on our website about the [properties that can be calculated](#) with Thermo-Calc and the Add-on Modules. Additional resources are added on a regular basis so keep checking back or [subscribe to our newsletter](#).

Wunderlich [2017Wun] measured the surface tension of CMSX-10 superalloy in the liquid state by the oscillating drop method in a container-less electromagnetic processing device on board a parabolic flight airplane. Mohr [2020Moh] performed their measurements in the electromagnetic levitator on board the International Space Station. The comparison between these two measurements and our description is shown.

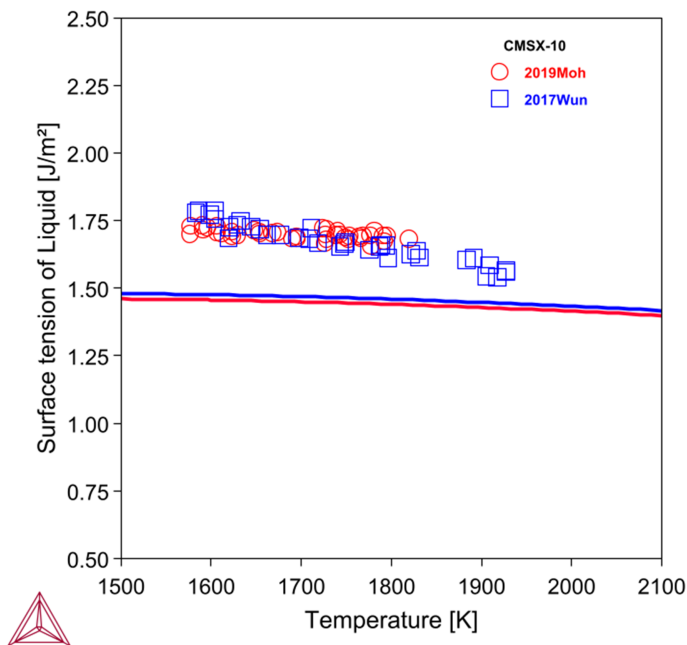


Figure 19: Calculated surface tension of CMSX10 superalloy along with experimental data from [2017Wun; 2020Moh].

References

- [2017Wun] R. K. Wunderlich, H.-J. Fecht, G. Lohöfer, Surface Tension and Viscosity of the Ni-Based Superalloys LEK94 and CMSX-10 Measured by the Oscillating Drop Method on Board a Parabolic Flight. *Metall. Mater. Trans. B.* 48, 237–246 (2017).
- [2020Moh] M. Mohr, R. Wunderlich, Y. Dong, D. Furrer, H.-J. Fecht, Thermophysical Properties of Advanced Ni-Based Superalloys in the Liquid State Measured on Board the International Space Station. *Adv. Eng. Mater.* 22, 1901228 (2020).

Viscosity of CMSX-10 Superalloy

The viscosity thermophysical property data is included with TCS Ni-based Superalloys Database (TCNI) starting with version 10 (TCNI10).

For more information about the various thermophysical models, and when in Thermo-Calc, press F1 to search the online help. The details are found under a *General Reference* section.



You can find information on our website about the [properties that can be calculated](#) with Thermo-Calc and the Add-on Modules. Additional resources are added on a regular basis so keep checking back or [subscribe to our newsletter](#).

Wunderlich [2017Wun] measured the viscosity of CMSX-10 superalloy by the oscillating drop method in a container-less electromagnetic processing device on board a parabolic flight airplane. Mohr [2020Moh] performed their measurements in the electromagnetic levitator on board the International Space Station. The comparison between these two measurements and our description is shown.

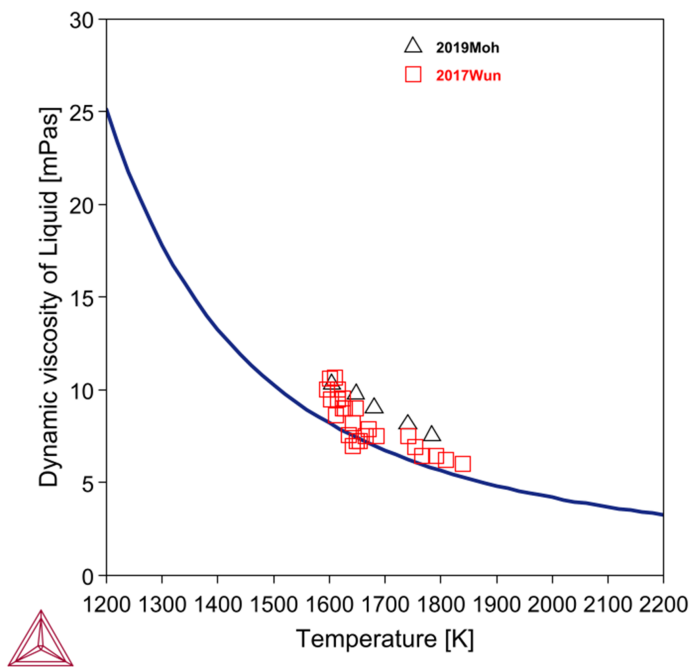


Figure 20: Calculated viscosity of CMSX10 along with experimental data.

References

[2017Wun] R. K. Wunderlich, H.-J. Fecht, G. Lohöfer, Surface Tension and Viscosity of the Ni-Based Superalloys LEK94 and CMSX-10 Measured by the Oscillating Drop Method on Board a Parabolic Flight. *Metall. Mater. Trans. B.* 48, 237–246 (2017).

[2020Moh] M. Mohr, R. Wunderlich, Y. Dong, D. Furrer, H.-J. Fecht, Thermophysical Properties of Advanced Ni-Based Superalloys in the Liquid State Measured on Board the International Space Station. Adv. Eng. Mater. 22, 1901228 (2020).

Electrical Resistivity of Some Commercial Alloys

Using the TCS Ni-based Superalloys Database (TCNI), you can calculate the quantities of a phase ϕ with the variable ELRS(ϕ) or a system (i.e. alloy) with ELRS. You can also calculate the derived quantity, i.e. electrical conductivity (ELCD) in a similar way.

The database includes electrical resistivity starting with version 11 (TCNI11).

For more information about the various thermophysical models, and when in Thermo-Calc, press F1 to search the online help. The details are found under a *General Reference* section.



You can find information on our website about the [properties that can be calculated](#) with Thermo-Calc and the Add-on Modules. Additional resources are added on a regular basis so keep checking back or [subscribe to our newsletter](#).

Ni-base Superalloy IN702

With the electrical resistivity described for most binary and several ternary systems, predictions can be made for multicomponent alloys, such as a Ni-base alloy IN702 in this example. The electrical resistivity of Ni-base alloys is usually in the order of $1e-6$ ohm-m.

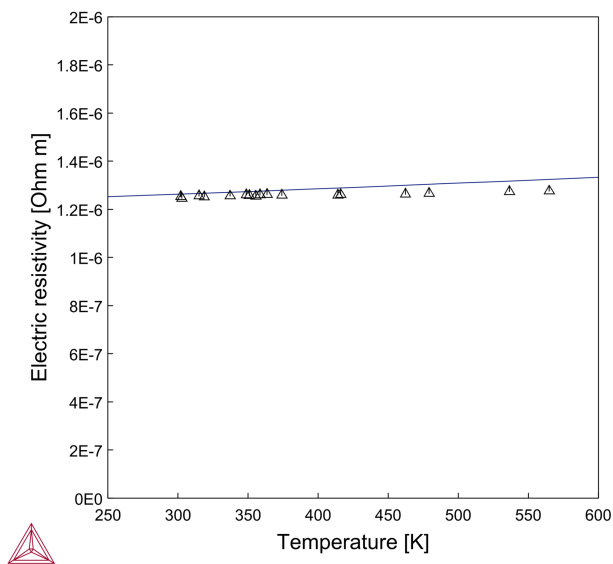


Figure 21: Electrical resistivity of alloy IN702 predicted using the Frozen-in Temperature Model available with the Property Model Calculator and compared with experimental data.

Commercial Ni-base Alloys

This example shows the predicted electrical resistivity of several commercial Ni-base alloys. The values are calculated by freezing-in the state at the typical annealing temperature of manufacture for each alloy. Deviations are expected, since the treatment of a material is not always known in the literature, and materials can have wide ranges of typical treatment temperatures.

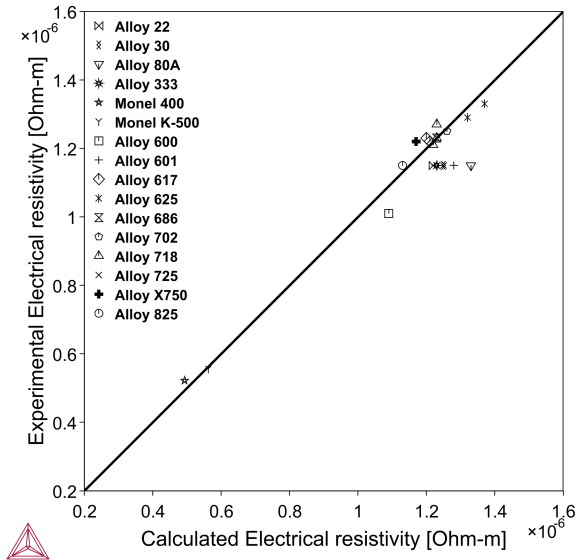


Figure 22: Parity plot comparing calculated with experimental electrical resistivity of various Ni-base superalloys at room temperature.



Read more on our website about [Property Models](#), including information about the Steel and Nickel Model Libraries, as well as how to create your own custom models in TC-Python. If you are in Thermo-Calc, press F1 to search the help.

Thermal Conductivity of Some Commercial Alloys

Using the TCS Ni-based Superalloys Database (TCNI), you can calculate the quantities of a phase ϕ with the variable THCD(ϕ), or a system (i.e. alloy) with THCD. You can also calculate the derived quantities, i.e. thermal resistivity (THRS) and thermal diffusivity (THDF), in a similar way.

The database includes thermal conductivity starting with version 11 (TCNI11).

For more information about the various thermophysical models, and when in Thermo-Calc, press F1 to search the online help. The details are found under a *General Reference* section.



You can find information on our website about the [properties that can be calculated](#) with Thermo-Calc and the Add-on Modules. Additional resources are added on a regular basis so keep checking back or [subscribe to our newsletter](#).

Ni-base Superalloy IN702

With the thermal conductivity described for most binary and several ternary systems, predictions can be made for multicomponent alloys, such as a Ni-base alloy IN702 in this example. The thermal conductivity of Ni-base alloys is usually in the range 10-20 W/mK.

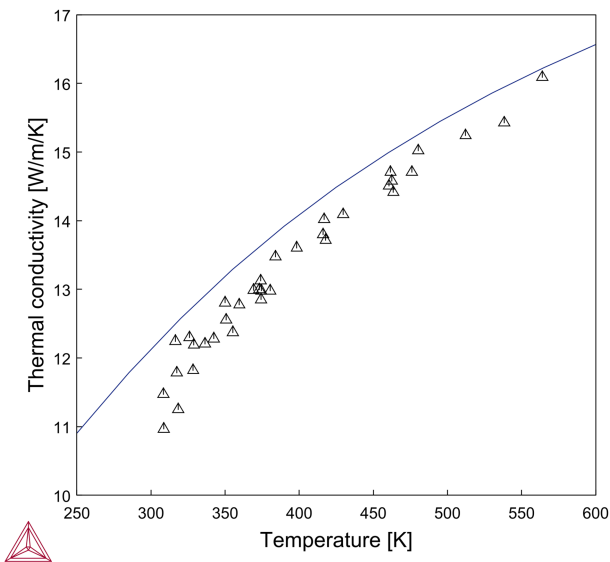


Figure 23: Thermal conductivity of alloy IN702 predicted using the Frozen-in Temperature Model available with the Property Model Calculator and compared with experimental data.

Commercial Ni-base Alloys

This example shows the predicted thermal conductivity of several commercial Ni-base alloys. The values are calculated by freezing-in the state at the typical annealing temperature of manufacture for each alloy. Deviations are expected, since the treatment of a material is not always known in the literature, and materials can have wide ranges of typical treatment temperatures.

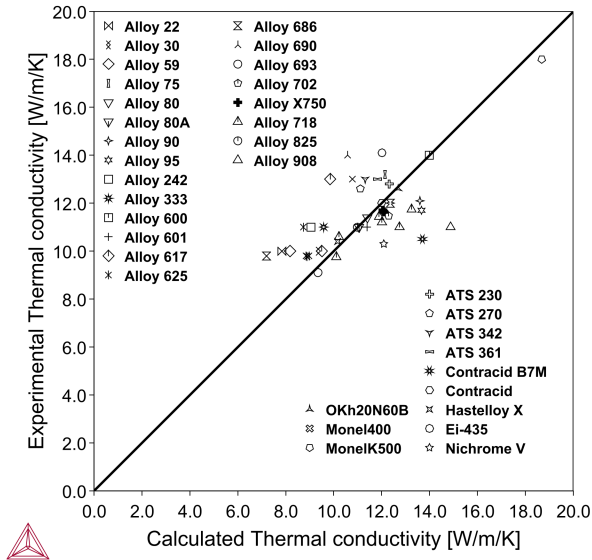


Figure 24: Parity plot comparing calculated with experimental thermal conductivity of various Ni-base superalloys at room temperature.



Read more on our website about [Property Models](#), including information about the Steel and Nickel Model Libraries, as well as how to create your own custom models in TC-Python. If you are in Thermo-Calc, press F1 to search the help.

TCNI Calculation Examples



Some of these phase diagrams are calculated with earlier versions of the database, so negligible differences might be observed if these are recalculated with the most recent version. The diagrams are updated where there is considerable or significant improvements.

In this section:

Binary Phase Diagrams	31
Ternary Isothermal Phase Diagram Sections	33
Prediction of Stable Phases	36
Prediction of Phase Stability with Minor Amounts of P in Ni-base Superalloys	38
Heat Treatment of a GTD111 Alloy	40
Precipitation and Coarsening of a 718 Alloy	42
Surface Tension: Cu-Fe, Fe-Ni, Cu-Ni, and Cu-Fe-Ni	45
Viscosity: Fe-Ni, Cr-Ni, and Cr-Fe-Ni	48
Electrical Resistivity: Co-Ni, Co-Fe, Co-Fe-Ni, and Higher Order Systems	51
Thermal Conductivity: Co-Ni, Co-Fe, and Co-Fe-Ni	54

Binary Phase Diagrams

Every binary system in the TCS Ni-based Superalloys Database (TCNI) is assessed to accurately describe experimental phase diagram data available in the literature.



Learn more on our website about the [CALPHAD Method](#) and how it is applied to the Thermo-Calc databases.



When working in Thermo-Calc with binary diagrams you use either the Binary Calculator (in Graphical Mode) or the Binary module (in Console Mode). The fundamental calculation engine is the same but you access the settings in different ways.

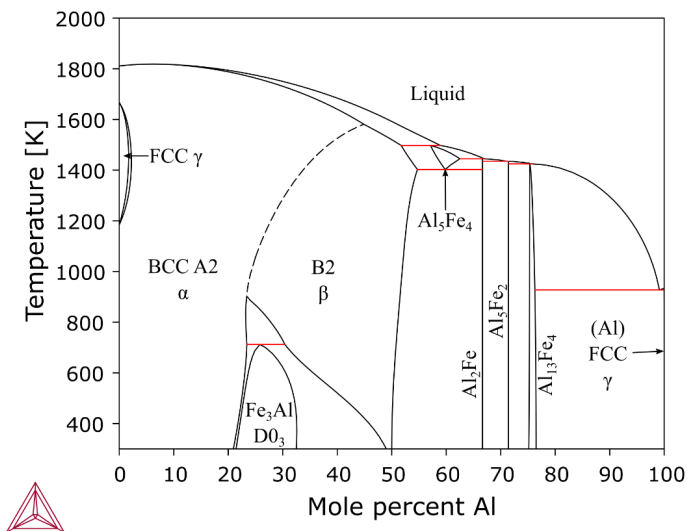


Figure 25: Phase diagram calculated for the Al-Fe system [1993Sei].

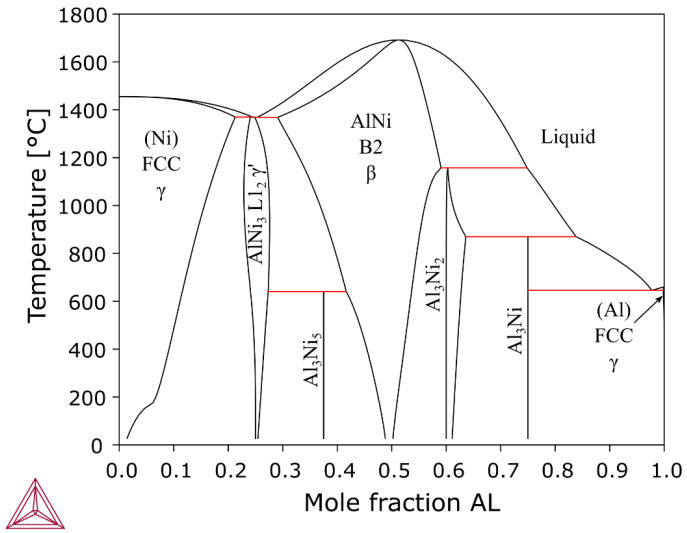


Figure 26: Phase diagram calculated for the Al-Ni system [1997Ans].

References

[1993Sei] E. M. Seiersten, Sintef report STF28F93051, (1993).

[1997Ans] I. Ansara, N. Dupin, H. L. Lukas, B. Sundman, Thermodynamic assessment of the Al-Ni system. J. Alloys Compd. 247, 20–30 (1997).

Ternary Isothermal Phase Diagram Sections

Many ternary systems pertaining to Ni-base superalloys are assessed to fit experimental data available in literature. These examples using the TCS Ni-based Superalloys Database (TCNI) are of calculated ternary isothermal phase diagram sections.



Learn more on our website about the [CALPHAD Method](#) and how it is applied to the Thermo-Calc databases.



When working in Thermo-Calc with ternary diagrams you use either the Ternary Calculator (in Graphical Mode) or the Ternary module (in Console Mode). The fundamental calculation engine is the same but you access the settings in different ways.

Al-Cr-Ni

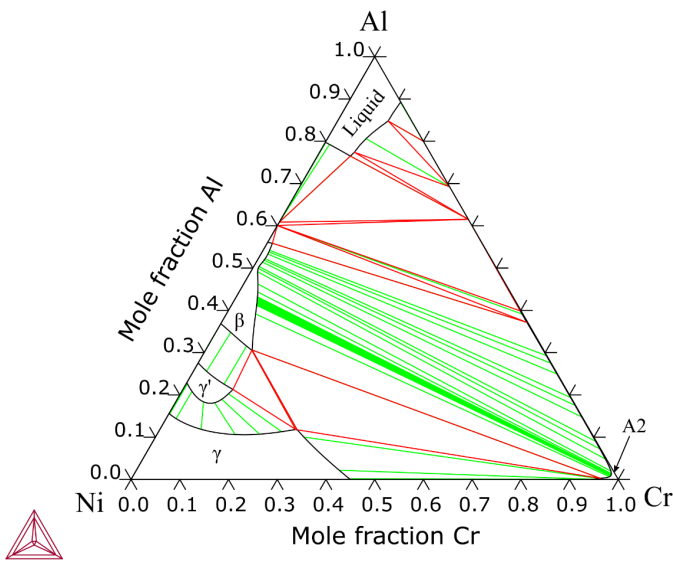


Figure 27: Isothermal section of the Al-Cr-Ni system [2001Dup] calculated at 1273 K.

Ni-Re-W

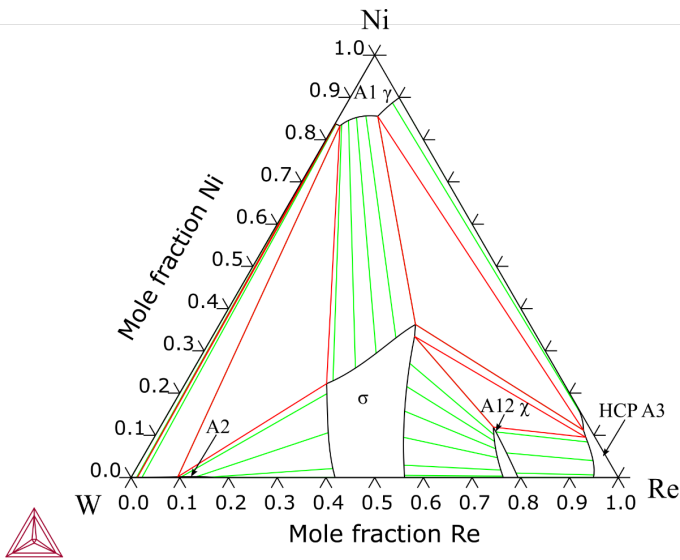


Figure 28: Isothermal section of the Ni-Re-W system calculated at 1273 K.

Co-Cr-Mo

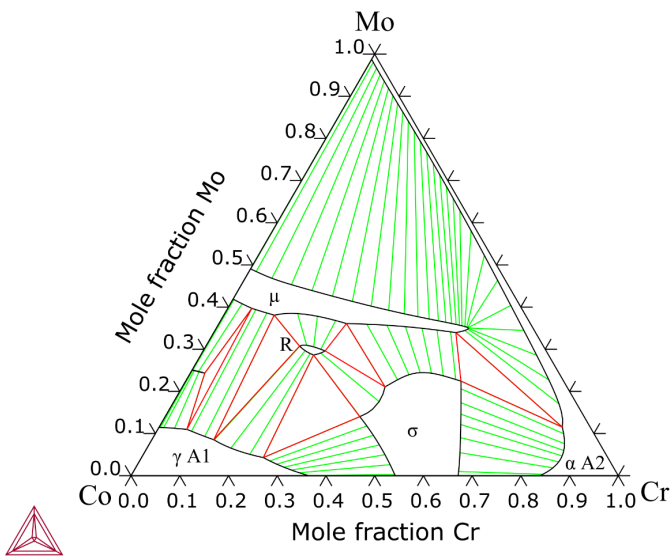


Figure 29: Isothermal section of the Co-Cr-Mo system calculated at 1273 K.

Mo-Ni-Re

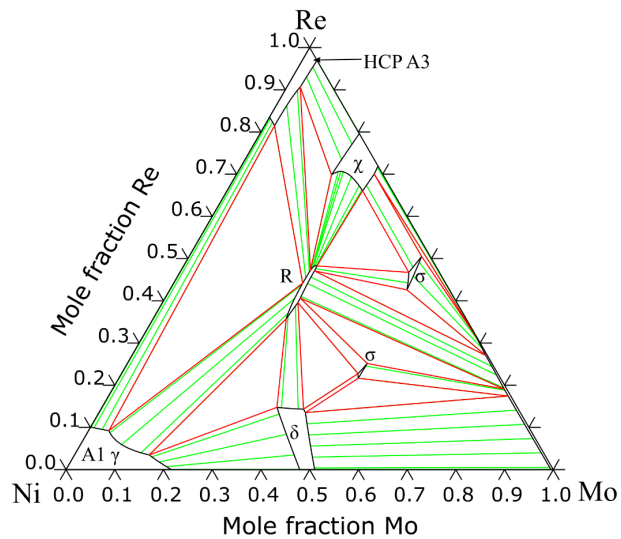


Figure 30: Isothermal section of the Mo-Ni-Re system calculated at 1273 K.

Nb-Ni-Ti

- $x_1 = \text{Nb}_{13}\text{Ni}_{75}\text{Ti}_{12}$
- $x_2 = \text{Nb}_5\text{Ni}_{75}\text{Ti}_{20}$
- $x_3 = \text{Nb}_{15}\text{Ni}_{56}\text{Ti}_{29}$
- $x_4 = \text{Nb}_{15}\text{Ni}_{80}\text{Ti}_{5}$
- $x_5 = \text{Nb}_8\text{Ni}_9\text{Ti}_3$

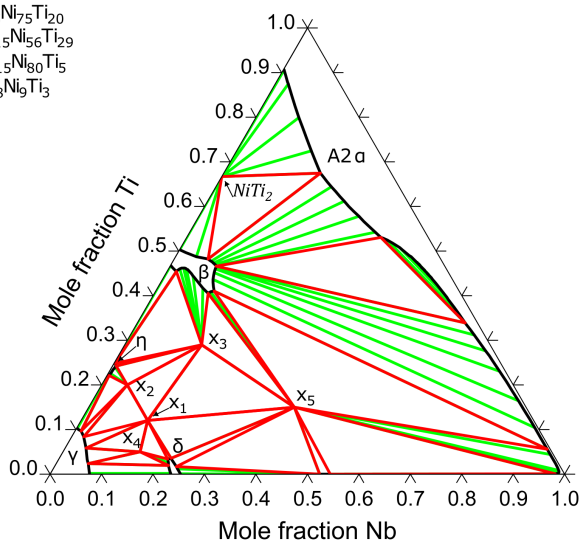


Figure 31: Isothermal section of the Nb-Ni-Ti system calculated at 1173 K.

Reference

[2001Dup] N. Dupin, I. Ansara, B. Sundman, Thermodynamic re-assessment of the ternary system Al-Cr-Ni. *Calphad*. 25, 279–298 (2001).

Prediction of Stable Phases

With so many binary and ternary systems assessed, many multicomponent alloys can be accurately described with the TCS Ni-based Superalloys Database (TCNI). These examples calculate the metastable phases in an 718-type alloy when the stable δ phase is suspended.

■ Ni-18Cr-18Fe-3Mo-0.5Al-1Ti-5.3Nb-0.02C Alloy

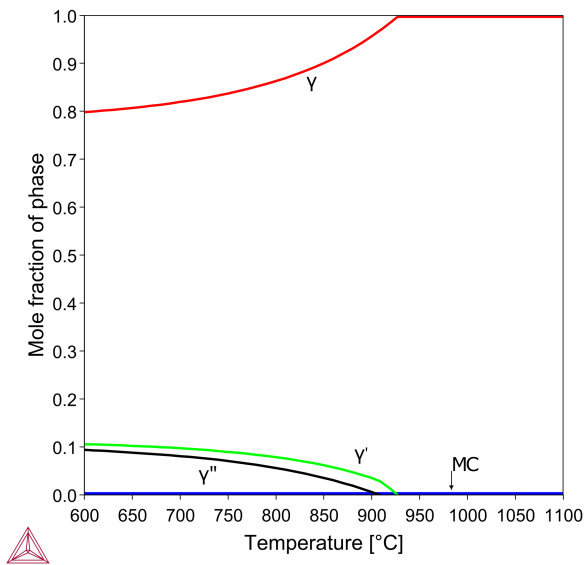


Figure 32: Predicted amount of phases (metastable calculation) at varying temperatures for a Ni-18Cr-18Fe-3Mo-0.5Al-1Ti-5.3Nb-0.02C (wt. %) alloy.

Ni-10Cr-5Al

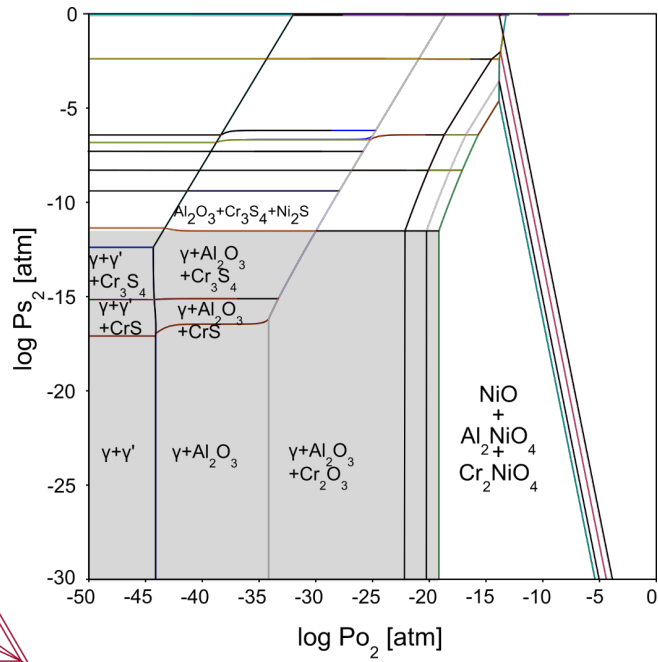


Figure 33: Calculated phase stability diagram of Ni-10Cr-5Al in the presence of SO_2 gas at 600 °C.

Prediction of Phase Stability with Minor Amounts of P in Ni-base Superalloys

These examples using the TCS Ni-based Superalloys Database (TCNI) include the use of the recently added element, phosphorus (P).



For other examples using P, see [Isothermal Solidification During Brazing: A Diffusion Simulation](#) and [Predicting Phase Stability: Applications Involving P](#).

In [Figure 34](#) the plot shows the volume fraction of phases versus temperature, for a Ni-Cr-Fe-C alloy with 0.09 wt% P added. Experimental studies have found M3P and M23C6 precipitates in such alloys, water-quenched after solutioning at 1100 °C [2019Lia], both of which are predicted to be stable at lower temperature in the calculation.

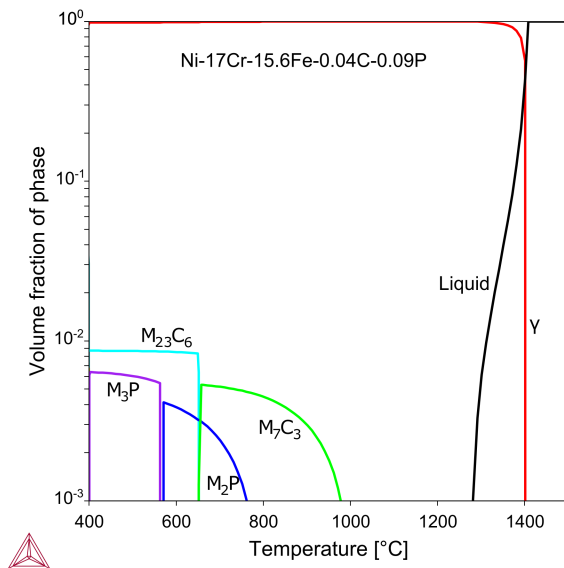


Figure 34: Volume fraction of phases as a function of temperature for a Ni-Cr-Fe-C-P alloy, showing M3P and M23C6 phases found in the literature [2019Lia].

A similar calculation is shown in [Figure 35](#) for alloy 706 with 0.025 wt% P added. Here we see a predicted presence of M2P C37-type phosphide phase, which is found in the literature in samples quenched from high temperature and then soaked at 980 °C, as a result of segregation of P in grain boundaries. The calculation is metastable; the stable sluggish phases are suspended to promote the typical γ'/γ'' phases.

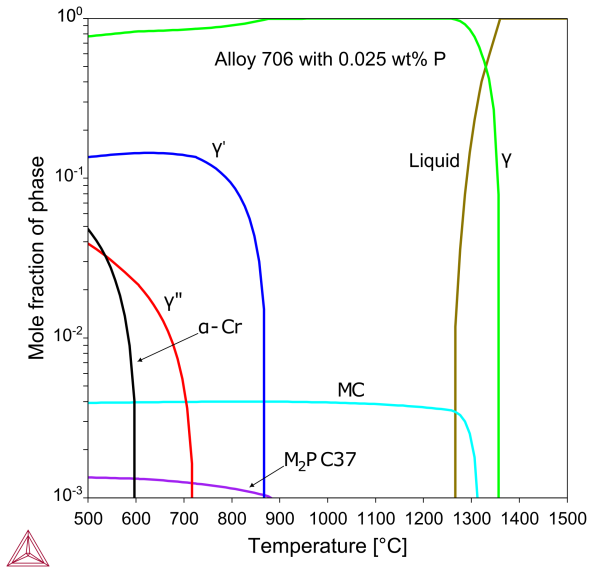


Figure 35: Mole fraction of phases as a function of temperature for a IN706 alloy with 0.025 wt% P, showing the prediction of the C37 phosphide, as found in the literature [2017Zha].

Reference

- [2017Zha] S. Zhang, L. Huang, A. Zhang, L. Yu, X. Xin, W. Sun, X. Sun, Segregation of Phosphorus and Precipitation of MNP-Type Phosphide at the Grain Boundary of IN706 Superalloy. *J. Mater. Sci. Technol.* 33, 187–191 (2017).
- [2019Lia] X.-T. Lian, W.-R. Sun, F. Liu, D.-D. Zheng, X. Xin, Effects of Phosphorus and Iron on Microstructures and Mechanical Properties in NiCrFe-Based Alloys. *Acta Metall. Sin. (English Lett.* 32, 659–667 (2019).

Heat Treatment of a GTD111 Alloy

The add-on Diffusion Module (DICTRA) can be used to simulate diffusion and phase transitions in selected regions of materials during heat treatments. Below is an example using the TCS Ni-based Superalloys Database (TCNI) to simulate the heat treatment of a GTD111 alloy with an Al-Ni B2 coating for 96 hours at 1050 °C. The simulation regards a 500 nm region of coating on a 500 nm region of sample.



Read more about the [Diffusion Module \(DICTRA\)](#) on our website. If you are in Thermo-Calc, press F1 to search the help to learn about the available settings included with the Add-on Module.

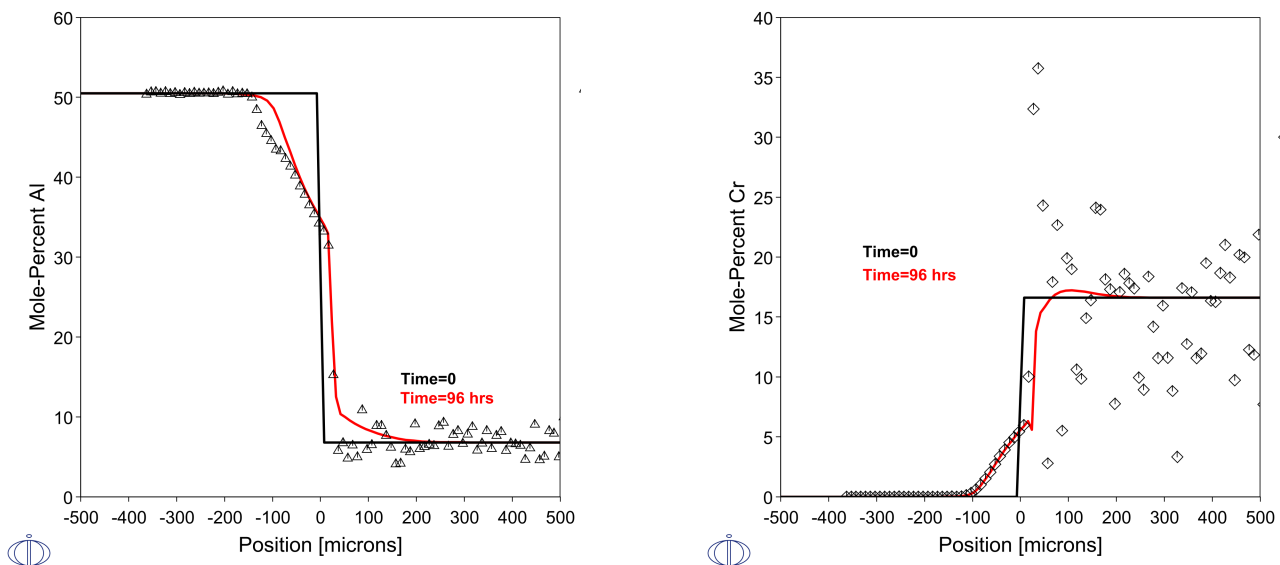


Figure 36: Diffusion Module (DICTRA) results from the simulation of a GTD111 alloy with B2 coating for 96 hours at 1050 °C, showing the evolution of the profile of (left) Al composition and (right) Cr composition both compared with experimental data by [2006Per].

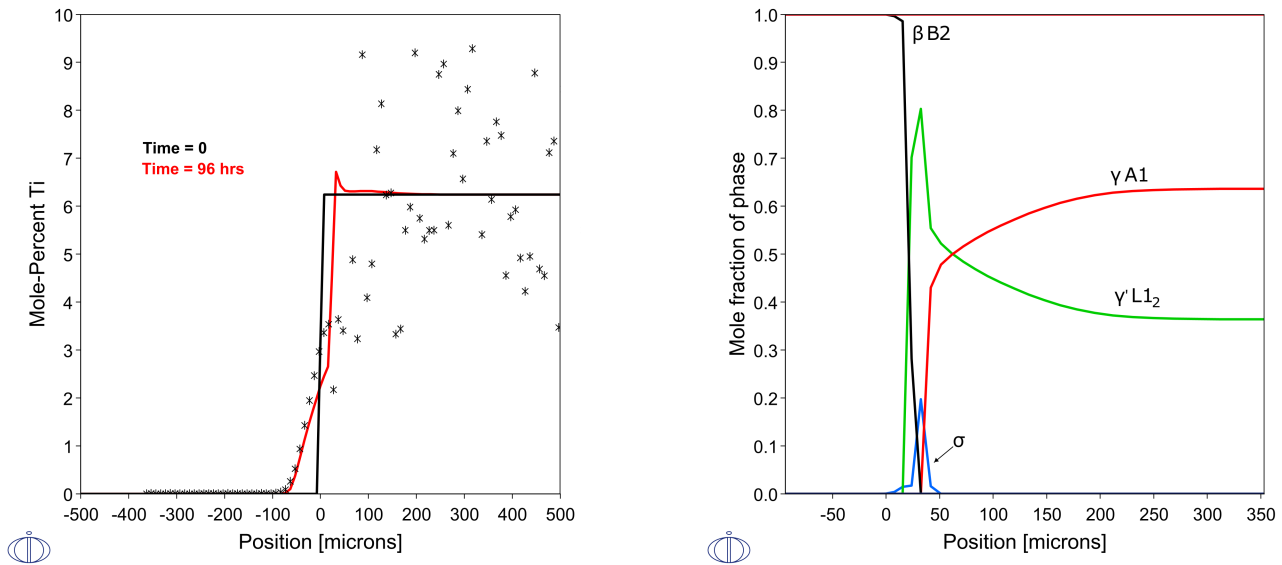


Figure 37: Diffusion Module (DICTRA) results from the simulation of a GTD111 alloy with B2 coating for 96 hours at 1050 °C, showing (left) the evolution of the profile of Ti composition, which is compared with experimental data by [2006Per] and (right) is the present phases at the final time of simulation.

Reference

[2006Per] E. Perez, T. Patterson, Y. Sohn, Interdiffusion analysis for NiAl versus superalloys diffusion couples, *J. Phase Equilibria Diffus.* 27, 659–664 (2006).

Precipitation and Coarsening of a 718 Alloy

The Precipitation Module (TC-PRISMA) can be used to simulate co-precipitation and coarsening of precipitates, shown below using the TCS Ni-based Superalloys Database (TCNI) and TCS Ni-alloys Mobility Database (MOBNI) for 718-type alloys.



Read more about the [Precipitation Module \(TC-PRISMA\)](#) on our website. If you are in Thermo-Calc, press F1 to search the help to learn about the available settings included with the Add-on Module.

As part of the simulation set up, these Precipitation Calculator settings are used in the calculation:

- **Cubic elastic properties in matrix phase**

- $c_{11} = 232.5$ GPa
- $c_{12} = 136.6$ GPa
- $c_{44} = 120$ GPa

- **Interfacial energy**

- $\gamma'' = 0.014$ J/m²
- $\gamma' = 0.14076 - 0.00012 * T$

- **Transformation strain**

- $\gamma'' : \epsilon_{11} = \epsilon_{22} = 0.00667$
- $\epsilon_{33} = 0.0286$



Results of particle size are sensitive to the value of interfacial energy.

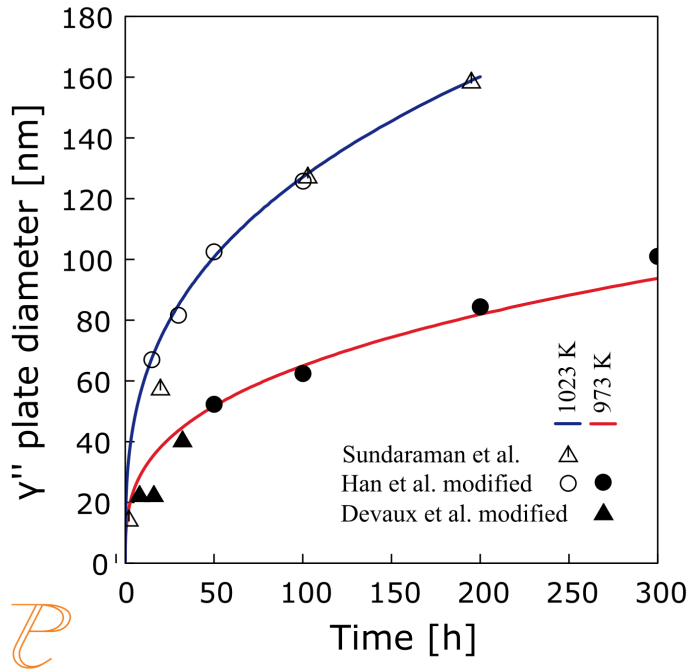


Figure 38: Calculated plate diameter/particle length of γ'' precipitates in 718 alloy compared with data in the literature [1982Han; 1992Sun; 2008Dev]. Where "modified" indicates that literature data was doubled with the possibility that reported values are half the major axis, as noted by [2018Wu].

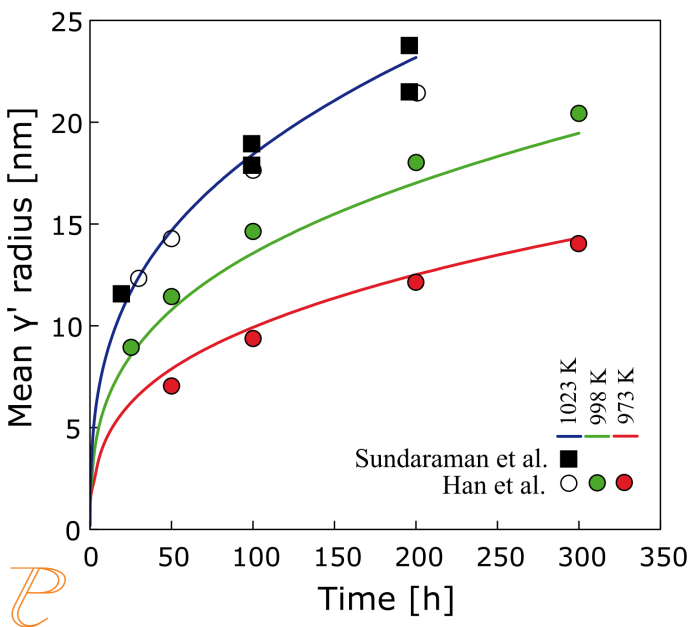


Figure 39: Mean γ' particle radius in 718-type alloy compared with data by [199Sun] at 1023 K, and [1982Han] at 998 and 973 K.

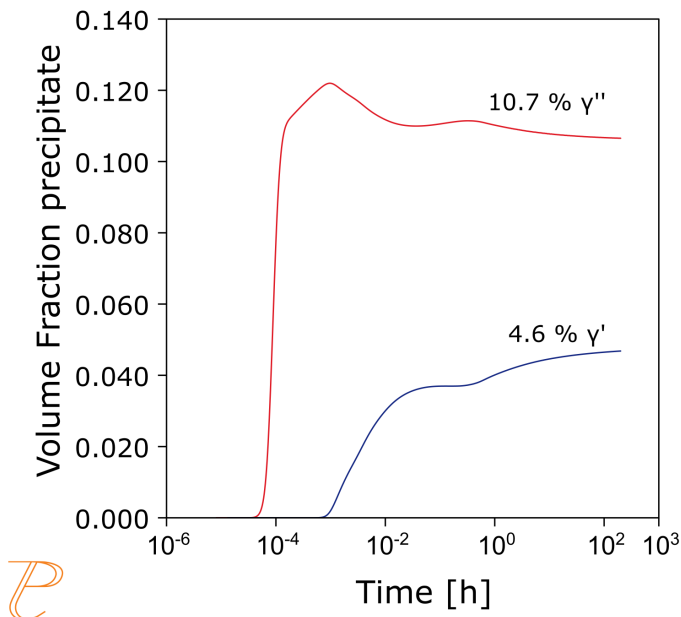


Figure 40: Volume fraction of precipitates simulated for 718-type alloy at 1023 K for 200 hours for a composition based on [1992Sun]. Note that time scale is logarithmic.

References

- [1982Han] Y. Han, P. Deb, M. C. Chaturvedi, Coarsening behaviour of γ'' - and γ' -particles in Inconel alloy 718, *Met. Sci.* 16(12), 555–562 (1982).
- [1992Sun] M. Sundararaman, P. Mukhopadhyay, S. Banerjee, Some aspects of the precipitation of metastable intermetallic phases in INCONEL 718, *Metall. Trans. A.* 23, 2015–2028 (1992).
- [2008Dev] A. Devaux, L. Nazé, R. Molins, A. Pineau, A. Organista, J. Y. Guédou, J. F. Uginet, P. Héritier, Gamma double prime precipitation kinetic in Alloy 718. *Mater. Sci. Eng. A.* 486, 117–122 (2008).
- [2018Wu] K. Wu, Q. Chen, P. Mason, Simulation of Precipitation Kinetics with Non-Spherical Particles. *J. Phase Equilibria Diffus.* 39, 571–583 (2018).

Surface Tension: Cu-Fe, Fe-Ni, Cu-Ni, and Cu-Fe-Ni

The surface tension thermophysical property data is included with the TCS Ni-based Superalloys Database (TCNI) starting with version 10 (TCNI10).

For more information about the various thermophysical models, and when in Thermo-Calc, press F1 to search the online help. The details are found under a *General Reference* section.



You can find information on our website about the [properties that can be calculated](#) with Thermo-Calc and the Add-on Modules. Additional resources are added on a regular basis so keep checking back or [subscribe to our newsletter](#).

Cu-Fe, Fe-Ni, and Cu-Ni

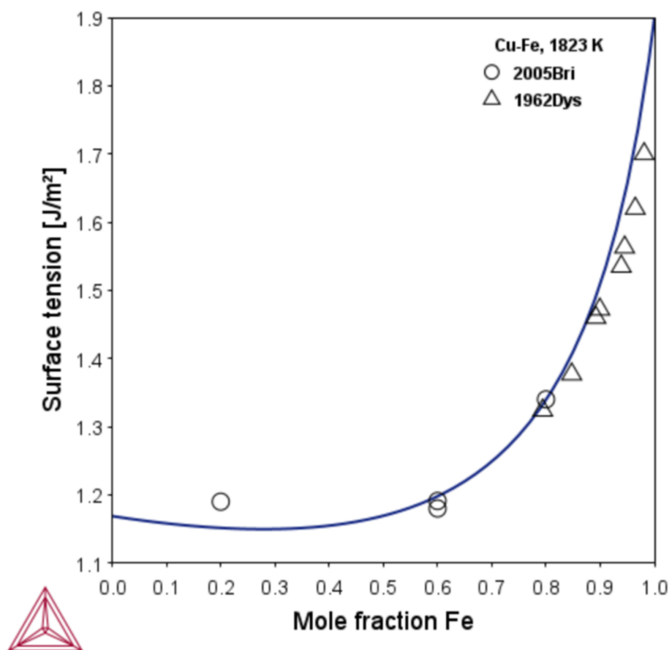


Figure 41: Calculated surface tension of Cu-Fe liquid binary alloy. The experimental data are taken from [1993Lee; 2005Bri; 2005Egr].

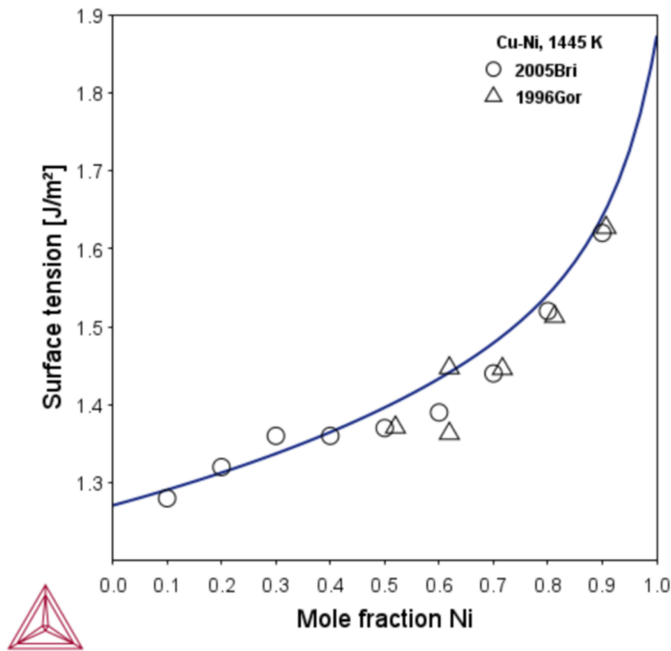


Figure 42: Calculated surface tension of Cu-Ni liquid binary alloy. The experimental data are taken from [1993Lee; 2005Bri; 2005Egr].

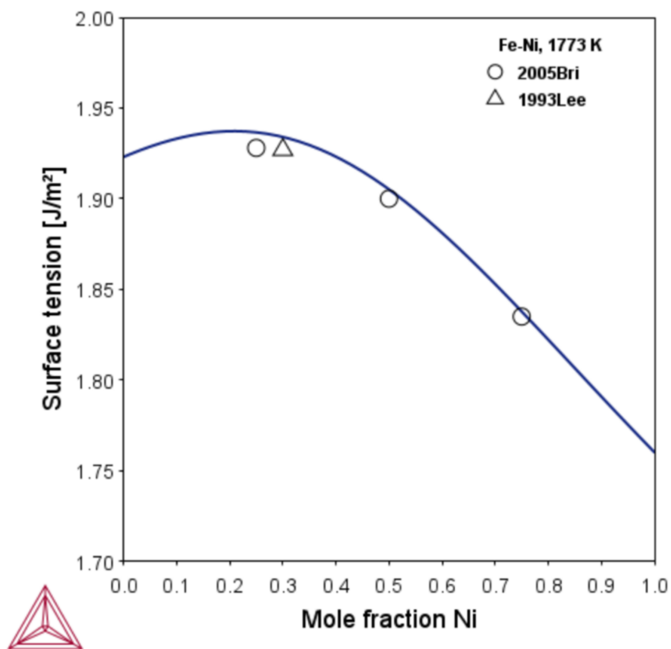


Figure 43: Calculated surface tension of Fe-Ni liquid binary alloy. The experimental data are taken from [1993Lee; 2005Bri; 2005Egr].

Cu-Fe-Ni

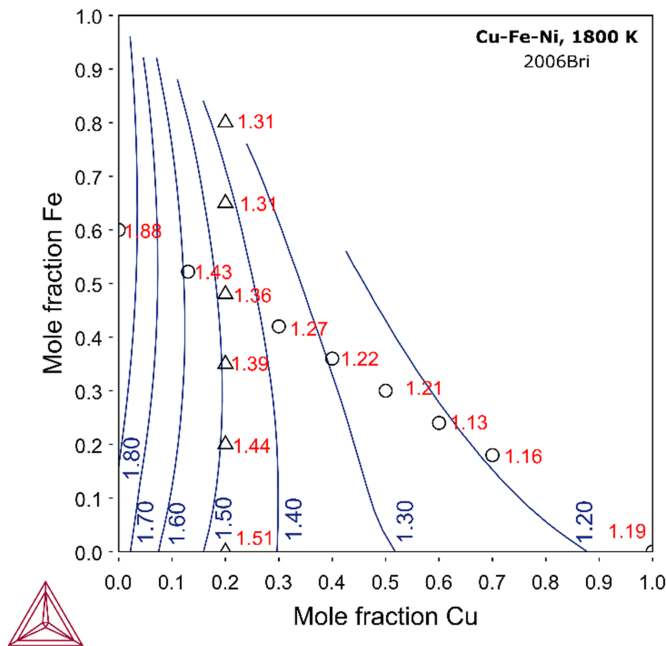


Figure 44: Calculated surface tension of Cu-Fe-Ni liquid ternary alloys. The experimental data are taken from [2006Bri].

References

- [1993Lee] H.-K. Lee, M. G. Froberg, J. P. Hajra, The determination of the surface tensions of liquid iron, nickel and iron-nickel alloys using the electromagnetic oscillating droplet technique. *Steel Res.* 64, 191–196 (1993).
- [2005Bri] J. Brillo, I. Egrý, Surface tension of nickel, copper, iron and their binary alloys. *J. Mater. Sci.* 40, 2213–2216 (2005).
- [2005Egr] I. Egrý, J. Brillo, T. Matsushita, Thermophysical properties of liquid Cu–Fe–Ni alloys. *Mater. Sci. Eng. A.* 413–414, 460–464 (2005).
- [2006Bri] J. Brillo, I. Egrý, T. Matsushita, Density and Surface Tension of Liquid Ternary Ni–Cu–Fe Alloys. *Int. J. Thermophys.* 27, 1778–1791 (2006).

Viscosity: Fe-Ni, Cr-Ni, and Cr-Fe-Ni

The viscosity thermophysical property data is included with TCS Ni-based Superalloys Database (TCNI) starting with version 10 (TCNI10).

For more information about the various thermophysical models, and when in Thermo-Calc, press F1 to search the online help. The details are found under a *General Reference* section.



You can find information on our website about the [properties that can be calculated](#) with Thermo-Calc and the Add-on Modules. Additional resources are added on a regular basis so keep checking back or [subscribe to our newsletter](#).

Fe-Ni and Cr-Ni

The calculated dynamic viscosity plots of Fe-Ni and Cr-Ni binary systems at 1873 K are shown.

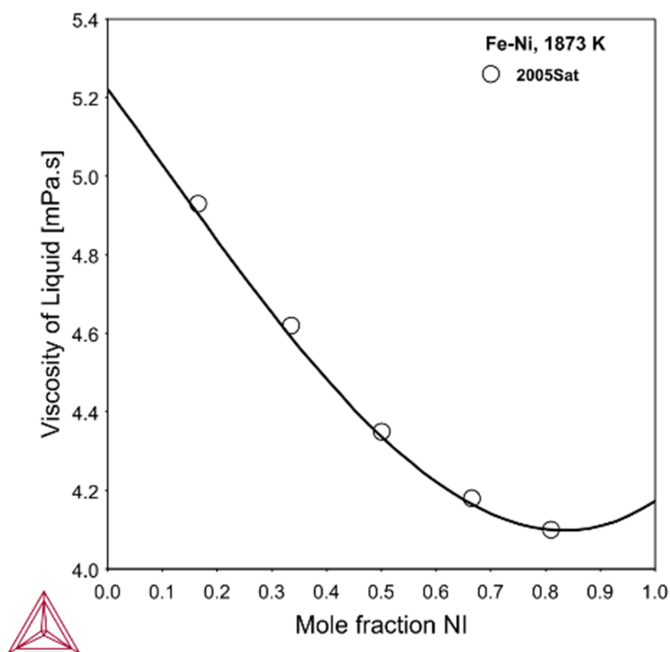


Figure 45: Isoviscosity curve for Fe-Ni system at 1873 K. Experimental data is from [2011Sat].

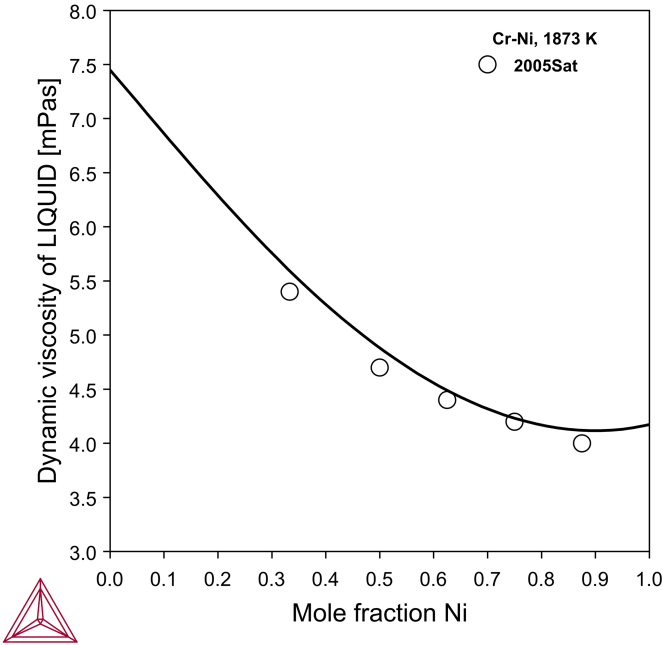


Figure 46: Isoviscosity curve of Cr-Ni system at 1873 K. Experimental data is from [2011Sat].

Cr-Fe-Ni

The isoviscosity curves of the Cr-Fe-Ni ternary system at 1800 K is shown.

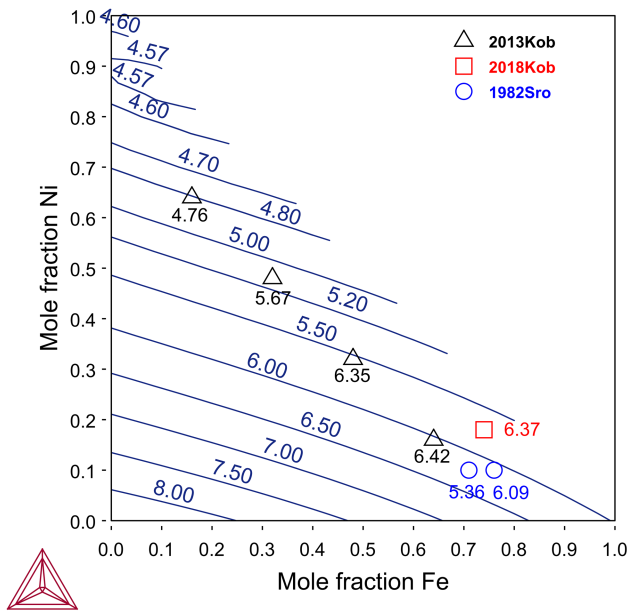


Figure 47: Isoviscosity of Cr-Fe-Ni at 1800 K. The viscosity values are in milli-Pascal. Second. Experimental data is from [2013Kob; 2018Kob].

References

- [2011Sat] Y. Sato, Representation of the Viscosity of Molten Alloy as a Function of the Composition and Temperature. *Jpn. J. Appl. Phys.* 50, 11RD01 (2011).
- [2013Kob] H. Kobatake, J. Brillo, Density and viscosity of ternary Cr-Fe-Ni liquid alloys. *J. Mater. Sci.* 48, 6818–6824 (2013).
- [2018Kob] H. Kobatake, J. Brillo, Surface tension and viscosity measurement of ternary Cr-Fe-Ni liquid alloys measured under microgravity during parabolic flights. *High Temp. -- High Press.* 47, 465–477 (2018).

Electrical Resistivity: Co-Ni, Co-Fe, Co-Fe-Ni, and Higher Order Systems

Using the TCS Ni-based Superalloys Database (TCNI), you can calculate the quantities of a phase ϕ with the variable ELRS(ϕ) or a system (i.e. alloy) with ELRS. You can also calculate the derived quantity, i.e. electrical conductivity (ELCD) in a similar way.

The database includes electrical resistivity starting with version 11 (TCNI11).

For more information about the various thermophysical models, and when in Thermo-Calc, press F1 to search the online help. The details are found under a *General Reference* section.



You can find information on our website about the [properties that can be calculated](#) with Thermo-Calc and the Add-on Modules. Additional resources are added on a regular basis so keep checking back or [subscribe to our newsletter](#).

The examples are a sample of calculated electrical resistivity for binary, ternary, and higher-order systems important to Ni-base alloys, compared to values from the literature.

Co-Ni

The electrical resistivity of the Co-Ni FCC solution for varying composition and temperature is compared with experimental data from the literature.

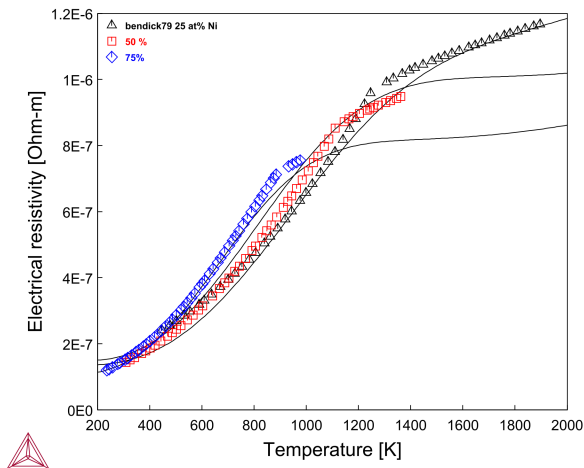


Figure 48: Calculated electrical resistivity for $\text{Co}_{25}\text{Ni}_{75}$, CoNi , and $\text{Co}_{75}\text{Ni}_{25}$ compared with experimental data [1979Ben].

Co-Fe

The calculated electrical resistivity for FCC-Co with up to 8 at% Fe dissolved, compared with experimental data from the literature. Since data is only available for a limited composition range, an approximate fit is deemed good enough with a relatively simple model.

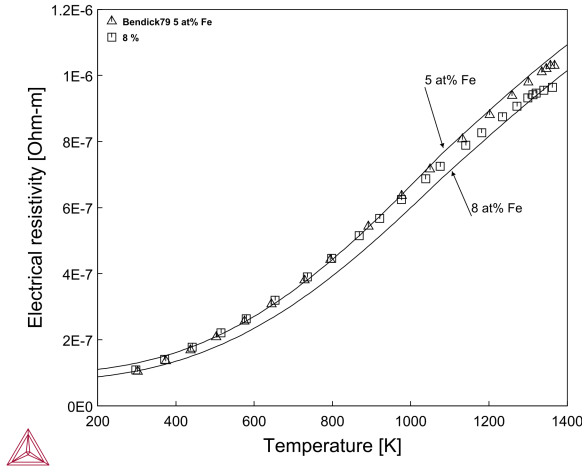


Figure 49: Calculated electrical resistivity of $Co_{95}Fe_5$ and $Co_{92}Fe_8$ alloys, compared with experimental data [1979Ben].

Co-Fe-Ni

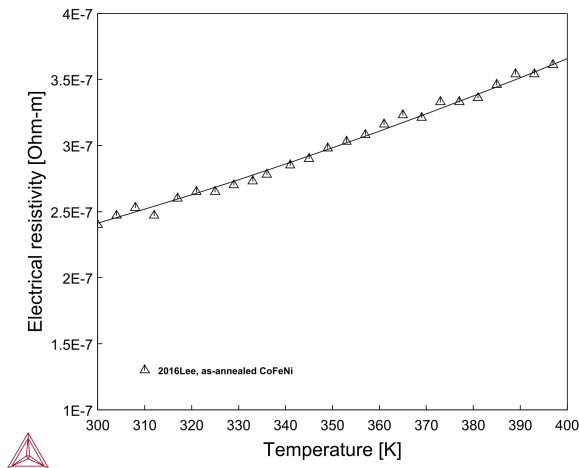


Figure 50: Calculated electrical resistivity of equiatomic Co-Fe-Ni compared with experimental data [2016Lee].

Parity of Electrical Resistivity of Selected Systems

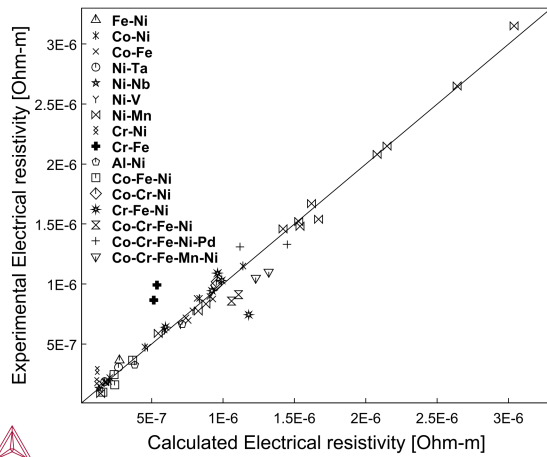


Figure 51: Parity plot showing calculated vs experimental electrical resistivity of binaries and higher order systems.

References

- [1979Ben] W. Bendick, H. H. Ettwig, W. Pepperhoff, Thermally excited electron transitions in FCC iron alloys. *J. Magn. Magn. Mater.* 10, 214–216 (1979).
- [2016Lee] J. I. Lee, H. S. Oh, E. S. Park, Manipulation of σ/κ ratio in single phase FCC solid-solutions. *Appl. Phys. Lett.* 109, 061906 (2016).

Thermal Conductivity: Co-Ni, Co-Fe, and Co-Fe-Ni

Using the TCS Ni-based Superalloys Database (TCNI), you can calculate the quantities of a phase ϕ with the variable THCD(ϕ), or a system (i.e. alloy) with THCD. You can also calculate the derived quantities, i.e. thermal resistivity (THRS) and thermal diffusivity (THDF), in a similar way.

The database includes thermal conductivity starting with version 11 (TCNI11).

For more information about the various thermophysical models, and when in Thermo-Calc, press F1 to search the online help. The details are found under a *General Reference* section.



You can find information on our website about the [properties that can be calculated](#) with Thermo-Calc and the Add-on Modules. Additional resources are added on a regular basis so keep checking back or [subscribe to our newsletter](#).

The examples are a sample of calculated thermal conductivity for binary, ternary, and higher-order systems important to Ni-base alloys, compared to experimental values from the literature.

Co-Ni

This plot shows the thermal conductivity of the Co-Ni FCC solution, for varying composition and temperature, compared with experimental data from the literature.

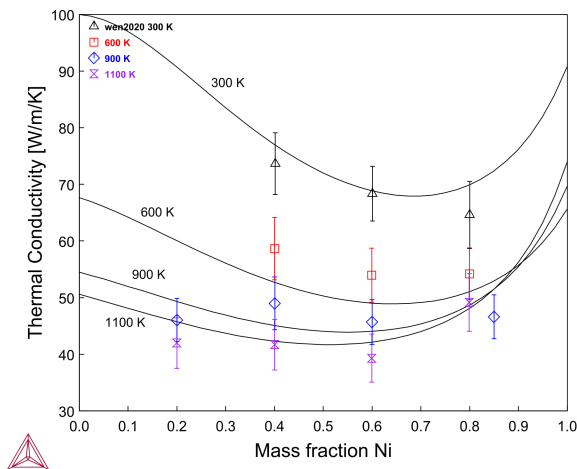


Figure 52: Calculated thermal conductivity of Co-Ni alloys at different temperatures and compositions, compared with experimental data [2020Wen].

Co-Fe

This is an example of the calculated thermal conductivity for FCC-Co with up to 8 at% Fe dissolved, compared with estimated data from the literature. Since data is only available for a limited composition range, an approximate fit is deemed good enough with a relatively simple model. Here the thermal conductivity is estimated using the Wiedemann-Franz law based on the electrical resistivity data, therefore discrepancies are expected.

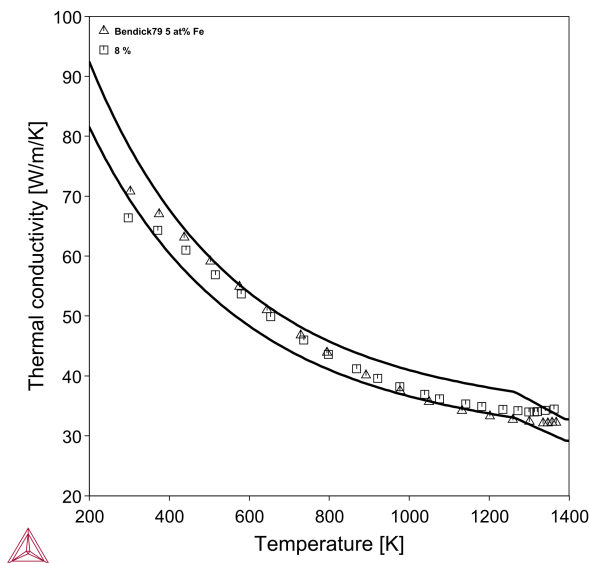


Figure 53: Calculated thermal conductivity for $Co_{95}Fe_5$ and $Co_{92}Fe_8$ alloys compared with estimated data points [1979Ben].

Co-Fe-Ni

The calculated thermal conductivity of the Co-Fe-Ni system compared to experimental data from the literature.

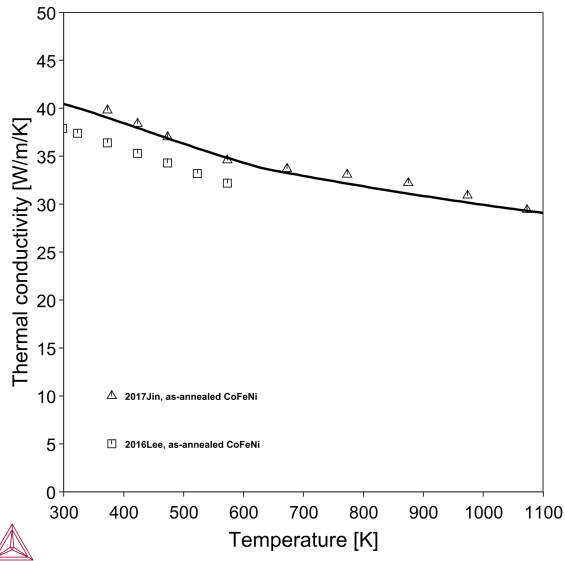


Figure 54: Calculated thermal conductivity of equiatomic Co-Fe-Ni compared with experimental data [2016Lee; 2017Jin].

Parity of Thermal Conductivity of Selected Systems

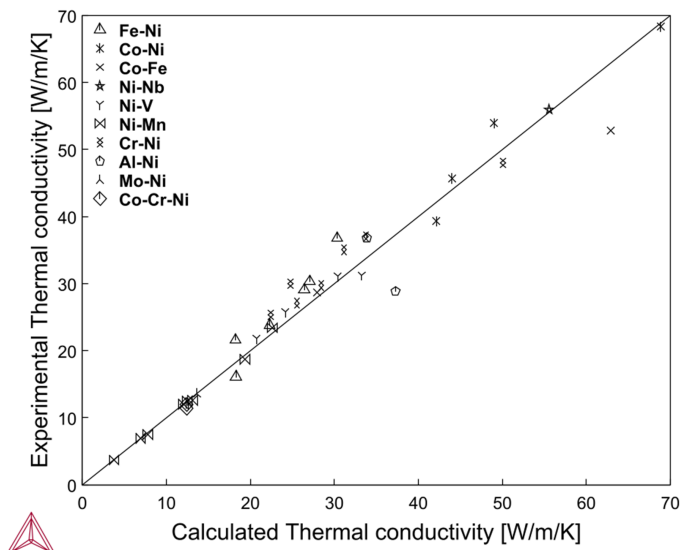


Figure 55: Parity plot showing calculated vs experimental thermal conductivity of binaries.

References

- [1979Ben] W. Bendick, W. Pepperhoff, Thermally excited states in cobalt and cobalt alloys. *J. Phys. F Met. Phys.* 9, 2185–2194 (1979).
- [2016Lee] J. I. Lee, H. S. Oh, E. S. Park, Manipulation of σ/κ ratio in single phase FCC solid-solutions. *Appl. Phys. Lett.* 109, 061906 (2016).

- [2017Jin] K. Jin, S. Mu, K. An, W. D. Porter, G. D. Samolyuk, G. M. Stocks, H. Bei, Thermophysical properties of Ni-containing single-phase concentrated solid solution alloys. *Mater. Des.* 117, 185–192 (2017).
- [2020Wen] S. Wen, Y. Liu, G. Kaptay, Y. Du, A new model to describe composition and temperature dependence of thermal conductivity for solution phases in binary alloys. *J. Mater. Sci. Technol.* 59, 72–82 (2020).